
LEARNING DAGS FROM DATA WITH FEW ROOT CAUSES

A PREPRINT

Panagiotis Misiakos, Chris Wendler and Markus Püschel

Department of Computer Science, ETH Zurich
{pmisiakos, wendlerc, markusp}@ethz.ch

May 26, 2023

ABSTRACT

We present a novel perspective and algorithm for learning directed acyclic graphs (DAGs) from data generated by a linear structural equation model (SEM). First, we show that a linear SEM can be viewed as a linear transform that, in prior work, computes the data from a dense input vector of random valued root causes (as we will call them) associated with the nodes. Instead, we consider the case of (approximately) few root causes and also introduce noise in the measurement of the data. Intuitively, this means that the DAG data is produced by few data-generating events whose effect percolates through the DAG. We prove identifiability in this new setting and show that the true DAG is the global minimizer of the L^0 -norm of the vector of root causes. For data with few root causes, with and without noise, we show superior performance compared to prior DAG learning methods.

1 Introduction

We consider the problem of learning the edges of an unknown directed acyclic graph (DAG) given data indexed by its nodes. DAGs can represent causal dependencies (edges) between events (nodes) in the sense that an event only depends on its predecessors. Thus, DAG learning has applications in causal discovery, which, however, is a more demanding problem that we do not consider here, as it requires further concepts of causality analysis, in particular interventions [Peters et al., 2017]. However, DAG learning is still NP-hard in general [Chickering et al., 2004]. Hence, in practice, one has to make assumptions on the data generating process, to infer information about the underlying DAG in polynomial time. Recent work on DAG learning has focused on identifiable classes of causal data generating processes. A frequent assumption is that the data follow a structural equation model (SEM) [Shimizu et al., 2006, Zheng et al., 2018, Gao et al., 2021], meaning that the value of every node is computed as a function of the values of its direct parents plus noise. A prominent example of DAG learning is NOTEARS [Zheng et al., 2018], which considers the class of linear SEMs and translates the acyclicity constraint into a continuous form for easier optimization. It inspired subsequent works to use continuous optimization schemes for both linear [Ng et al., 2020] and nonlinear SEMs [Lachapelle et al., 2019, Zheng et al., 2020]. A more expansive discussion of related work is provided in Section 4.

In this paper we also focus on linear SEMs but change the data generation process. We first translate the common representation of a linear SEM as recurrence into an equivalent closed form. In this form, prior data generation can be viewed as linearly transforming an i.i.d. random, dense vector of root causes (as we will call them) associated with the DAG nodes as input into the actual data on the DAG nodes as output. Then we impose sparsity in the input (few root causes) and introduce measurement noise in the output. Intuitively, this assumption captures the reasonable situation that DAG data may be mainly determined by few data generation events of predecessor nodes that percolate through the DAG as defined by the linear SEM.

Contributions. We provide a novel DAG learning method designed for DAG data generated by linear SEMs with the novel assumption of few root causes. Our specific contributions include the following:

- We provide an equivalent, closed form of the linear SEM equation showing that it can be viewed as a linear transform obtained by the reflexive-transitive closure of the DAGs adjacency matrix. In this form, prior data generation assumed a dense, random vector as input, which we call root causes.

- In contrast, we assume a sparse input, or few root causes (with noise) that percolate through the DAG to produce the output, whose measurement is also subject to noise.
- We prove identifiability of our proposed setting under weak assumptions. We also show that, given enough data, the original DAG is the unique minimizer of the associated optimization problem in the case of absent noise.
- We propose a novel and practical DAG learning algorithm, called SparseRC, for our setting, based on the minimization of the L^1 -norm of the approximated root causes.
- We benchmark SparseRC against prior DAG learning algorithms, showing significant improvements for synthetic data with few root causes and scalability to thousands of nodes. SparseRC also performs among the best on real data from a gene regulatory network, demonstrating that the assumption of few root causes can be relevant in practice.

2 Linear SEMs and Root Causes

We first provide background on prior data generation for directed acyclic graphs (DAGs) via linear SEMs. Then we present a different viewpoint on linear SEMs based on the concept of root causes that we introduce. Based on it, we argue for data generation with few root causes, present it mathematically, and motivate it, including with a real-world example.

DAG. We consider DAGs $\mathcal{G} = (V, E)$ with $|V| = d$ vertices, E the set of directed edges, no cycles including no self-loops. We assume the vertices to be sorted topologically and set accordingly $V = \{1, 2, \dots, d\}$. Further, $a_{ij} \in \mathbb{R}$ is the weight of edge $(i, j) \in E$, and

$$\mathbf{A} = (a_{ij})_{i,j \in V} = \begin{cases} a_{ij}, & \text{if } (i, j) \in E, \\ 0, & \text{else.} \end{cases} \quad (1)$$

is the weighted adjacency matrix. \mathbf{A} is upper triangular with zeros on the diagonal and thus $\mathbf{A}^d = \mathbf{0}$.

Linear SEM.

Linear SEMs [Peters et al., 2017] formulate a data-generating process for DAGs \mathcal{G} . First, the values at the sources of a \mathcal{G} are initialized with random noise. Then, the remaining nodes are processed in topological order: the value x_j at node j is assigned the linear combination of its parents' values (called the causes of x_j) plus independent noise. Mathematically, a data vector $\mathbf{x} = (x_1, \dots, x_d)^T \in \mathbb{R}^d$ on \mathcal{G} follows a linear SEM if $x_j = \mathbf{x}^T \mathbf{A}_{:,j} + n_j$, where the subscript $:, j$ denotes column j , and n_j are i.i.d. random noise variables [Shimizu et al., 2006, Zheng et al., 2018, Ng et al., 2020]. Assuming n such data vectors collected as the rows of a matrix $\mathbf{X} \in \mathbb{R}^{n \times d}$, and the noise variables in the matrix \mathbf{N} , the linear SEM is typically written as

$$\mathbf{X} = \mathbf{X}\mathbf{A} + \mathbf{N}. \quad (2)$$

2.1 Transitive closure and root causes

Equation (2) can be viewed as a recurrence for computing the data values \mathbf{X} from \mathbf{N} . Here, we interpret linear SEMs differently by first solving this recurrence in closed form. We define $\overline{\mathbf{A}} = \mathbf{A} + \mathbf{A}^2 + \dots + \mathbf{A}^{d-1}$, which is the Floyd-Warshall (FW) transitive closure of \mathbf{A} over the ring $(\mathbb{R}, +, \cdot)$ [Lehmann, 1977], and $\mathbf{I} + \overline{\mathbf{A}}$ the associated reflexive-transitive closure of \mathbf{A} . Since $\mathbf{A}^d = \mathbf{0}$ we have $(\mathbf{I} - \mathbf{A})(\mathbf{I} + \overline{\mathbf{A}}) = \mathbf{I}$ and thus can isolate \mathbf{X} in (2):

Theorem 2.1. *The linear SEM (2) computes data \mathbf{X} as*

$$\mathbf{X} = \mathbf{N}(\mathbf{I} + \overline{\mathbf{A}}). \quad (3)$$

In words, the data values in \mathbf{X} are computed as linear combinations of the noise values \mathbf{N} of all predecessor nodes with weights given by the reflexive-transitive closure $\mathbf{I} + \overline{\mathbf{A}}$.

Since \mathbf{X} is uniquely determined by \mathbf{N} , we call the latter the *root causes* of \mathbf{X} .

Few root causes. In (3) we view \mathbf{N} as the input to the linear SEM at each node and \mathbf{X} as the measured output at each node. With this viewpoint we argue that it makes sense to consider a data generation process that differs in two ways from (3) and thus (2). First, we assume that only few nodes produce a relevant input that we call \mathbf{C} , up to low magnitude noise \mathbf{N}_c . Second, we assume that the measurement of \mathbf{X} is subject to noise \mathbf{N}_x . Formally, this yields the closed form

$$\mathbf{X} = (\mathbf{C} + \mathbf{N}_c)(\mathbf{I} + \overline{\mathbf{A}}) + \mathbf{N}_x. \quad (4)$$

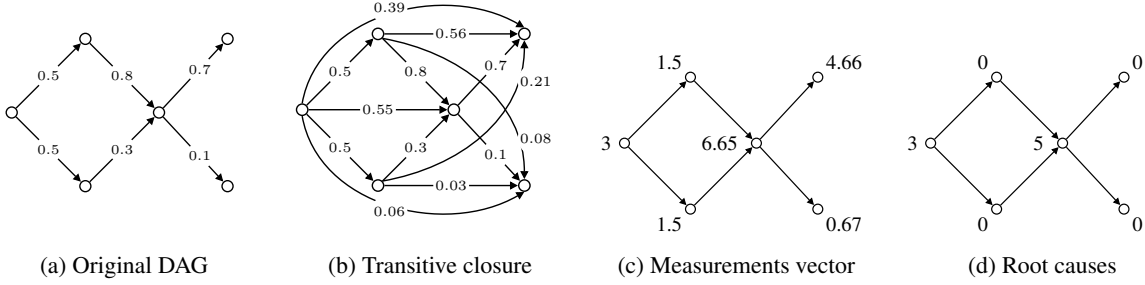


Figure 1: (a) A DAG for a river network. The weights capture fractions of pollution transported between adjacent nodes. (b) The transitive closure. The weights are fractions of pollution transported between all pairs of connected nodes. (c) A possible vector measuring pollution, and (d) the root causes of the pollution, sparse in this case.

Multiplying both sides by $(\mathbf{I} + \overline{\mathbf{A}})^{-1} = (\mathbf{I} - \mathbf{A})$ yields the (standard) form as recurrence

$$\mathbf{X} = \mathbf{X}\mathbf{A} + (\mathbf{C} + \mathbf{N}_c) + \mathbf{N}_x (\mathbf{I} - \mathbf{A}), \quad (5)$$

i.e., \mathbf{N} in (2) is replaced by $\mathbf{C} + \mathbf{N}_c + \mathbf{N}_x (\mathbf{I} - \mathbf{A})$. Note that (4) generalizes (3), which is obtained by assuming zero root causes $\mathbf{C} = \mathbf{0}$ and zero measurement noise $\mathbf{N}_x = \mathbf{0}$.

We consider \mathbf{C} not as an additional noise variable but as the actual information, i.e., the relevant input data at each node, which then percolates through the DAG as determined by the SEM to produce the final output data \mathbf{X} , whose measurement, as usual in practice, is subject to noise. Few root causes means that only few nodes input relevant information in one dataset. Formally, \mathbf{C} is sparse and (\gg means significantly larger)

$$\begin{aligned} \min_{i,j} \{|c_{ij}|, c_{ij} \neq 0\} &\gg \max\{\|\mathbf{N}_c\|_\infty, \|\mathbf{N}_x\|_\infty\} \quad (\text{negligible noise}), \\ nd &\gg \|\mathbf{C}\|_0 \quad (\text{few root causes}), \end{aligned} \quad (6)$$

where the L^0 -pseudo-norm counts the nonzero entries of \mathbf{C} . Next we motivate our assumptions with a possible real-world example, that, in concept, can be transferred to other settings.

2.2 Example: Pollution model

Linear SEMs and associated algorithms have been extensively studied in the literature [Loh and Bühlmann, 2014, Peters and Bühlmann, 2014, Ghoshal and Honorio, 2017, Aragam and Zhou, 2015]. However, we are not aware of any real-world example given in a publication. The motivation for using linear SEMs includes the following two reasons. The first is that d -variate Gaussian distributions can always be expressed as linear SEMs [Aragam and Zhou, 2015] and the second that linearity is often a workable assumption when approximating non-linear systems.

Our aim is to explain why we propose the assumption of few root causes. The high-level intuition is that it can be reasonable to assume that, with the view point of (3), the relevant DAG data is triggered by sparse events on the input size and not by random noise. To illustrate this, we present a linear SEM that describes the propagation of pollution in a river network. The abstract idea that the weights of the edges express the fractions of the values that are propagated through the DAG can be transferred to other real-world scenarios.

DAG. We assume a DAG describing a river network. The acyclicity is guaranteed since flows only occur downstream. The nodes $i \in V$ represent geographical points of interest, e.g., cities, and edges are rivers connecting them. We assume that the cities can pollute the rivers. An edge weight $a_{ij} \in [0, 1]$, $(i, j) \in E$, captures what fraction of a pollutant inserted at i reaches the neighbour j . An example DAG with six nodes is depicted in Fig. 1a.

Transitive closure. Fig. 1b shows the transitive closure of the DAG in (a). The (i, j) -th entry of the transitive closure is denoted with \bar{a}_{ij} and represents the total fraction of a pollutant at i that reaches j via all connecting paths.

Data and root causes. Fig. 1c shows a possible data vector \mathbf{x} on the DAG, for example the pollution measurement at each node done once a day (and without noise in this case). The measurement is the accumulated pollution from all upstream nodes. Within the model, the associated root causes \mathbf{c} in Fig. 1d then show the origin of the pollution, two in this case. Sparsity in \mathbf{C} means that each day only a small number of cities pollute. Negligible pollution from other sources is captured by noise \mathbf{N}_c and \mathbf{N}_x models the noise in the pollution measurements.

3 Learning the DAG

In this section we present our approach for recovering the DAG adjacency matrix \mathbf{A} from given data \mathbf{X} under the assumption of few root causes, i.e., (4) (or (5)) and (6).

We first show that our proposed setting is identifiable. Then we theoretically analyze our data-generating model in the absence of noise and prove that the true DAG adjacency \mathbf{A} is the global minimizer of the L^0 -norm of the root causes. Finally, to learn the DAG in practice, we perform a continuous relaxation to obtain an optimization problem that is solvable with differentiation.

3.1 Identifiability

The rows of the data \mathbf{X} generated by a linear SEM are commonly interpreted as observations of a random row vector $X = (X_1, \dots, X_d)$ Peters and Bühlmann [2014], Zheng et al. [2018], i.e., it is written analogous to (2) as $X_i = X \mathbf{A}_{:,i} + N_i$, where N_i are i.i.d. zero-mean random noise variables, or, equivalently, as $X = X \mathbf{A} + N$. Given a distribution P_N of the noise vector, the DAG with graph adjacency matrix \mathbf{A} is then called identifiable if it is uniquely determined by the distribution P_X of X . One standard criterion from Shimizu et al. [2006] states that \mathbf{A} is identifiable if all N_i are non-Gaussian noise variables. This applies directly to our setting and yields the following result.

Theorem 3.1. *Assume the data generation $X = (C + N_c) (\mathbf{I} + \overline{\mathbf{A}}) + N_x$, where C, N_c and N_x are independent. Let $p \in [0, 1)$ and assume the C_i are independent random variables taking uniform values from $[0, 1]$ with probability p , and are $= 0$ with probability $1 - p$. The noise vectors N_c, N_x are defined as before. Then the DAG given by \mathbf{A} is identifiable.*

Proof. Using (5), the data generation equation can be viewed as a linear SEM (in standard recursive form) with noise variable $C + N_c + N_x (\mathbf{I} - \mathbf{A})$, which is non-Gaussian because C is non-Gaussian due to Lévy-Cramér decomposition theorem Lévy [1935], Cramér [1936]. The statement therefore follows from LiNGAM [Shimizu et al., 2006]. \square

In Theorem 3.1, C yields sparse observations whenever p is close to zero (namely dp root causes in expectation). However, identifiability follows for all p due to non-Gaussianity.

3.2 L^0 minimization problem and global minimizer

Suppose that the data \mathbf{X} are generated via the noise-free version of (4):

$$\mathbf{X} = \mathbf{C} (\mathbf{I} + \overline{\mathbf{A}}). \quad (7)$$

We assume \mathbf{C} to be generated as in Theorem 3.1, i.e., with randomly uniform values from $[0, 1]$ with probability p and 0 with probability $1 - p$, where p is small such that \mathbf{C} is sparse. Given the data \mathbf{X} we propose the following optimization problem to retrieve the DAG structure:

$$\min_{\mathbf{A} \in \mathbb{R}^{d \times d}} \left\| \mathbf{X} (\mathbf{I} + \overline{\mathbf{A}})^{-1} \right\|_0 \quad \text{s.t. } \mathbf{A} \text{ is acyclic.} \quad (8)$$

Among all possible DAG matrices, the solution of the optimization problem (8) is the one that minimizes the number of the root causes $\mathbf{X} (\mathbf{I} + \overline{\mathbf{A}})^{-1} = \mathbf{C}$.

The following Theorem 3.2 states that, given enough data, the solution of (8) is, with high probability, the true DAG given by \mathbf{A} and thus is the unique global minimizer of (8). One can view the result as a form of concrete, non-probabilistic identifiability. Note that Theorem 3.2 is not a sample-complexity result, but a statement of exact reconstruction in the absence of noise. The sample-complexity of our algorithm is empirically evaluated later.

Theorem 3.2. *Consider a DAG with weighted adjacency matrix \mathbf{A} . Given a large enough, but finite, number n of samples \mathbf{X} the matrix \mathbf{A} is, with high probability, the global minimizer of the optimization problem (8).*

Proof sketch. Given enough data n we can find, with high likelihood (approaching one as n increases), pairs of sub-matrices of root causes matrices \mathbf{C} (true) and $\widehat{\mathbf{C}}$ (corresponding to the solution of optimization), with the same support and covering all possibilities of support with k non-zero elements, due to the assumption of randomly varying support. Exploiting the support of the pairs we iteratively prove that the entries of the matrices \mathbf{A} (true) and $\widehat{\mathbf{A}}$ (solution of the optimization) are equal. The complete proof is provided in the supplementary material. \square

3.3 Continuous relaxation

In practice the optimization problem (8) is too expensive to solve due its combinatorial nature, and, of course, the noise-free assumption rarely holds in real-world data. We now consider again our general data generation in (4) assuming sparse root causes \mathbf{C} and noises $\mathbf{N}_c, \mathbf{N}_x$ satisfying the criterion (6). To solve it we consider a continuous relaxation of the optimization objective. Typically (e.g., Zheng et al. [2018], Lee et al. [2019], Bello et al. [2022]), continuous optimization DAG learning approaches have the following general formulation:

$$\begin{aligned} \min_{\mathbf{A} \in \mathbb{R}^{d \times d}} \ell(\mathbf{X}, \mathbf{A}) + R(\mathbf{A}) \\ \text{s.t.} \quad h(\mathbf{A}) = 0, \end{aligned} \quad (9)$$

where $\ell(\mathbf{A}, \mathbf{X})$ is the loss function corresponding to matching the data, $R(\mathbf{A})$ is a regularizer that promotes sparsity in the adjacency matrix, usually equal to $\lambda \|\mathbf{A}\|_1$, and $h(\mathbf{A})$ is a continuous constraint enforcing acyclicity.

In our case, following a common practice in the literature, we substitute the L^0 -norm from (8) with its convex relaxation [Ramirez et al., 2013], the L^1 -norm. We capture the acyclicity with the continuous constraint $h(\mathbf{A}) = \text{tr}(e^{\mathbf{A} \odot \mathbf{A}}) - d$ from [Zheng et al., 2018], could also take the form in [Yu et al., 2019]. As sparsity regularizer for the adjacency matrix and we choose $R(\mathbf{A}) = \lambda \|\mathbf{A}\|_1$. In practice, we found that our method works equally well in the absence of the regularizer ($\lambda = 0$). Hence, our final continuous optimization problem is

$$\min_{\mathbf{A} \in \mathbb{R}^{d \times d}} \frac{1}{2n} \left\| \mathbf{X} (\mathbf{I} + \overline{\mathbf{A}})^{-1} \right\|_1 \quad \text{s.t.} \quad h(\mathbf{A}) = 0. \quad (10)$$

We call this method SparseRC (sparse root causes).

4 Related work

The approaches to solving the DAG learning problem fall into two categories: combinatorial search or continuous relaxations. In general, DAG learning is an NP-hard problem since the combinatorial space of possible DAGs is super-exponential in the number of vertices [Chickering et al., 2004]. Thus, methods that search on the space of possible DAGs apply heuristic criteria to find an approximation of the ground truth DAG [Ramsey et al., 2017, Chickering, 2002, Tsamardinos et al., 2006].

Continuous optimization. Lately, with the advances of deep learning, researchers have been focusing on continuous optimization methods [Vowels et al., 2021] modelling the data generation process using SEMs. Among the first methods to utilize SEMs were CAM [Bühlmann et al., 2014] and LiNGAM [Shimizu et al., 2006], which specializes to linear SEMs with non-Gaussian noise. NOTEARS [Zheng et al., 2018] formulates the combinatorial constraint of acyclicity as a continuous one, which enables the use of standard optimization algorithms. Despite concerns, such as lack of scale-invariance [Kaiser and Sipos, 2022, Reisach et al., 2021], it has inspired many subsequent DAG learning methods. The current state-of-the-art of DAG learning methods for linear SEMs includes DAGMA Bello et al. [2022] which introduces a log-det acyclicity constraint and GOLEM [Ng et al., 2020] that studies the role of the weighted adjacency matrix sparsity, the acyclicity constraint, and proposes to directly minimize the data likelihood. A continuation of NOTEARS applies to non-linear SEMs [Zheng et al., 2020]. Other nonlinear methods for DAG learning include DAG-GNN [Yu et al., 2019], in which also a more efficient acyclicity constraint than the one in NOTEARS is proposed, and DAG-GAN [Gao et al., 2021]. DAG-NoCurl [Yu et al., 2021] proposes learning the DAG on the equivalent space of weighted gradients of graph potential functions. The method DYNOTEARS [Pamfil et al., 2020] implements a variation of NOTEARS compatible with time series data. A recent line of works considers permutation-based methods to parameterize the search space of the DAG [Charpentier et al., 2022, Zantedeschi et al., 2022]. Our work considers DAG learning under the new assumption of few root causes.

Fourier analysis. Our work is also related to the recently proposed form of Fourier analysis on DAGs from Seifert et al. [2022a,b], where equation (3) appears as a special case. The authors argue that (what we call) the root causes can be viewed as a form of spectrum of the DAG data. This means the assumption of few root causes is equivalent to Fourier-sparsity, a key concepts for prior forms of Fourier transform, including, classically, for the discrete Fourier transform (DFT) [Hassanieh, 2018], or the Walsh-Hadamard transform (WHT) for estimating set functions Stobbe and Krause [2012], Amrollahi et al. [2019].

Table 1: SHD metric (lower is better) for learning DAGs with 40 nodes and 80 edges. Each row is an experiment. The first row is the default, whose settings are in the blue column. In each other row, exactly one default parameter is changed (change). The last six columns correspond to prior algorithms. The best results are shown bold. Entries with SHD higher than 80 are reported as *failure*.

Hyperparameter	Default	Change	Varsort.	SparseRC (ours)	DAGMA	GOLEM	NOTEARS	DAG-NoCurl	GES	sortnregress
1. Default settings			0.96	0.00 ± 0.00	25.80 ± 3.71	2.70 ± 2.24	3.10 ± 2.30	28.20 ± 5.67	56.90 ± 25.84	failure
2. Graph type	Erdős-Renyi	Scale-free	0.99	0.00 ± 0.00	26.20 ± 4.79	1.10 ± 1.38	0.90 ± 0.94	7.60 ± 5.68	78.00 ± 39.52	33.30 ± 9.23
3. Edges / vertices	2	3	0.97	0.90 ± 1.04	44.40 ± 7.10	4.30 ± 2.87	10.40 ± 8.26	40.50 ± 14.02	failure	failure
4. Larger weights in \mathbf{A}	(0.4, 0.8)	(0.5, 2)	0.98	23.10 ± 13.66	13.80 ± 3.63	1.60 ± 3.26	8.50 ± 8.42	20.30 ± 8.53	64.30 ± 35.96	failure
5. High sparsity in \mathbf{C}	$p = 0.3$	$p = 0.1$	0.96	0.00 ± 0.00	65.70 ± 3.23	4.90 ± 4.28	9.80 ± 2.31	36.90 ± 7.78	47.40 ± 25.42	failure
6. Low sparsity in \mathbf{C}	$p = 0.3$	$p = 0.6$	0.96	64.80 ± 4.40	14.30 ± 4.22	2.50 ± 1.96	2.50 ± 1.36	32.30 ± 11.44	63.60 ± 25.05	failure
7. N_c, N_x deviation	$\sigma = 0.01$	$\sigma = 0.1$	0.96	3.50 ± 1.75	21.00 ± 2.53	2.50 ± 1.36	3.50 ± 2.50	26.40 ± 8.91	50.80 ± 13.37	75.40 ± 19.27
8. N_c, N_x distribution	Gaussian	Gumbel	0.96	0.20 ± 0.40	27.00 ± 3.29	4.10 ± 2.98	4.60 ± 3.38	24.30 ± 8.06	53.10 ± 21.19	failure
9. Measurement noise	$N_c \neq 0$ $N_x = 0$	$N_c = 0$ $N_x \neq 0$	0.96	0.10 ± 0.30	24.10 ± 3.70	3.40 ± 4.15	2.80 ± 1.72	30.10 ± 9.54	54.10 ± 18.25	failure
10. Full Noise	$N_c = 0$ $N_x = 0$	$N_c \neq 0$ $N_x \neq 0$	0.96	0.30 ± 0.64	27.50 ± 3.17	2.10 ± 1.51	4.00 ± 3.71	31.70 ± 8.15	69.10 ± 29.90	failure
11. Standardization	No	Yes	0.50	78.70 ± 3.93	62.70 ± 7.40	67.70 ± 8.99	79.60 ± 6.84	failure	41.80 ± 17.97	failure
12. Samples	n=1000	n = 20	0.92	failure	76.10 ± 4.72	failure	failure	failure	failure	error
13. Fixed support	No	Yes	0.87	failure	73.50 ± 4.18	failure	failure	failure	56.10 ± 8.25	failure

5 Experiments

We experimentally evaluate our DAG learning method SparseRC with both synthetically generated data with few root causes and real data from gene regulatory networks [Sachs et al., 2005].¹

Benchmarks. We compare against prior DAG learning methods suitable for data generated by linear SEMs with additive noise. In particular, we consider the prior DAGMA [Bello et al., 2022], GOLEM [Ng et al., 2020]², NOTEARS [Zheng et al., 2018], DAG-NoCurl [Yu et al., 2021], greedy equivalence search (GES) [Chickering, 2002], and the recent simple baseline sortnregress [Reisach et al., 2021]. We also compared SparseRC against LiNGAM Shimizu et al. [2006], fast greedy equivalence search (fGES) [Ramsey et al., 2017], max-min hill-climbing (MMHC) [Tsamardinos et al., 2006], and causal additive models (CAM) [Bühlmann et al., 2014], but they where not competitive and thus we only include the results in the supplementary material.

Metrics. To evaluate the found approximation $\hat{\mathbf{A}}$ of the true adjacency matrix \mathbf{A} , we use common performance metrics as in [Ng et al., 2020, Reisach et al., 2021]. In particular, the structural Hamming distance (SHD), which is the number of edge insertions, deletions, or reverses needed to convert $\hat{\mathbf{A}}$ to \mathbf{A} , and the structural intervention distance (SID), introduced by Peters and Bühlmann [2015], which is the number of falsely estimated intervention distributions. We also report the total number of nonzero edges (NNZ) discovered for the real dataset [Sachs et al., 2005] and, in addition, provide results reporting the true positive rate (TPR) and normalized mean square error (NMSE) metrics in the supplementary material. For each performance metric we compute the average and standard deviation over ten repetitions of the same experiment.

Our implementation. To solve (10) in practice, we implemented³ a PyTorch model with a trainable parameter representing the weighted adjacency matrix \mathbf{A} . This allows us to utilize GPUs for the acceleration of the execution of our algorithm (GOLEM uses GPUs, NOTEARS does not). Then we use the standard Adam [Kingma and Ba, 2014] optimizer to minimize the loss defined in (10).

5.1 Evaluation on data with few root causes

Data generating process and defaults. In the blue column of Table 1 we report the default settings for our experiment. We generate a random Erdős-Renyi graph with $d = 40$ nodes and assign edge directions to make it a DAG as in [Zheng et al., 2018]. The ratio of edges to vertices is set to 2, so the number of edges is 80. The entries of the weighted adjacency matrix are sampled uniformly at random from $(-b, -a) \cup (a, b)$, where $a = 0.4$ and $b = 0.8$. Following [Zheng et al., 2018, Ng et al., 2020, Bello et al., 2022] the result of the adjacency matrix approximation is post-processed for each algorithm by including only edges with absolute weight larger than a threshold $\omega = 0.3$. Next, the root causes \mathbf{C} are instantiated by setting each entry either to some random uniform value from $(0, 1)$ with probability $p = 0.3$ or to 0 with probability $1 - p = 0.7$ (thus, as in Theorem 3.1, the location of the root causes will vary). The data matrix \mathbf{X} is

¹We also mention that our method was among the winning solutions of a recent competition of DAG learning methods to infer causal relationships between genes [Chevalley et al., 2022]. The evaluation was done on non-public data by the organizing institution and is thus not included here.

²We use the equal variance formulation since we generate data with the same noise variance.

³All of our code is available as supplementary material. We used the repositories of [Bello et al., 2022], [Zheng et al., 2018], [Shimizu et al., 2006], [Yu et al., 2021] [Lachapelle et al., 2019], and the causal discovery toolbox [Kalainathan and Goudet, 2019].

Table 2: Runtime [seconds] report on the same settings of the top-performing methods.

Hyperparameter	Default value	Current value	SparseRC (ours)	GOLEM	NOTEARS
1. Default settings			4.63 ± 0.74	85.06 ± 2.26	7.68 ± 2.23
2. Graph type	Erdős-Renyi	Scale-free	4.98 ± 0.62	87.42 ± 4.97	3.54 ± 0.27
3. Edges / Vertices	2	3	5.68 ± 0.39	81.48 ± 1.10	22.47 ± 1.77
4. Larger weights in A	(0.4, 0.8)	(0.5, 2)	15.21 ± 1.50	91.93 ± 1.99	91.00 ± 52.95
5. High sparsity in C	$p = 0.3$	$p = 0.1$	4.17 ± 0.40	81.92 ± 1.32	3.98 ± 1.02
6. Low sparsity in C	$p = 0.3$	$p = 0.6$	6.51 ± 0.31	81.47 ± 1.64	9.78 ± 1.59
7. N_c, N_x deviation	$\sigma = 0.01$	$\sigma = 0.1$	6.11 ± 0.27	82.00 ± 1.04	9.04 ± 3.02
8. N_c, N_x distribution	Gaussian	Gumbel	4.68 ± 0.65	82.36 ± 2.01	7.46 ± 1.59
9. Measurement noise	$N_c \neq 0, N_x = 0$	$N_c = 0, N_x \neq 0$	4.92 ± 1.25	84.15 ± 1.79	6.16 ± 0.99
10. Full Noise	$N_c \neq 0, N_x = 0$	$N_c \neq 0, N_x \neq 0$	4.55 ± 0.38	81.92 ± 1.84	6.89 ± 1.05
11. Standardization	No	Yes	5.83 ± 0.32	81.98 ± 1.86	34.65 ± 4.93
12. Samples	$n=1000$	$n = 20$	4.95 ± 0.08	76.84 ± 1.60	30.61 ± 12.97
13. Fixed support	No	Yes	7.19 ± 0.17	102.49 ± 3.66	10.48 ± 6.56

computed according to (4), using Gaussian noise N_c, N_x of standard deviation $\sigma = 0.01$. By default we set $N_x = 0$, and consider $N_x \neq 0$ in a variant. The low standard deviation ensures that the inequalities (6) hold and that the data have approximately few root causes. Finally, we do not standardize (scaling for variance = 1) the data, and \mathbf{X} contains $n = 1000$ samples (number of rows).

Experiment 1: Different application scenarios. Table 1 compares SparseRC to six prior algorithms using the SHD metric. Every row corresponds to a different experiment that alters one particular hyperparameter of the default setting, which is the first row with values of the blue column as explained above. For example, the second row only changes the graph type from Erdős-Renyi to scale-free, while keeping all other settings. Note that in the last row, fixed support means that the location of the root causes is fixed for every sample in the data.

Since the graphs have 80 edges, an $\text{SHD} \ll 80$ can be considered as good and beyond 80 can be considered a failure. These cases are indicated as such in Table 1. Note that when the ratio edges/vertices is 3 (row 3) this threshold is set to 120. In Table 2 we also compare the runtimes of the overall most successful algorithms. SID and TPR comparison are shown in the supplementary material. Overall, SparseRC achieves very low SHD compared to other methods, is usually best and fastest, and sometimes even computes the exact solution, whereas none of the others does so.

First, we examine scenarios that alter the DAG configuration. For the default settings (row 1), for scale-free graphs (row 2), and for more edges (row 3) SparseRC performs best and perfectly (in row 3 almost) detects all edges. As in [Zheng et al., 2018, Ng et al., 2020] we consider different weights for the adjacency matrix to examine the sensitivity of the weight scale (row 4). We see that, larger weight bounds affect negatively our performance.

Next, we consider changing hyperparameters that affect the root causes and the data. Higher sparsity (fewer root causes) (row 5) keeps the performance perfect, whereas very low sparsity (row 6) degrades it significantly as expected. In contrast, imposing high sparsity is harmful for example for DAGMA, GOLEM and NOTEARS. Higher standard deviation in the root causes noise (row 7) decreases performance overall and SparseRC comes second close to GOLEM and NOTEARS. Changing to Gumbel noise (row 8) keeps the almost perfect performance. Applying noise only on the root causes or both on the measurements and root causes (rows 9 and 10) mostly maintains performance over all, including our almost perfect reconstruction. The standardization of data (row 11) is generally known to negatively affect algorithms with continuous objectives [Reisach et al., 2021] as is the case here for all. For a small number of samples (row 12) or fixed sparsity support (row 13) (practically) all methods fail. Overall, SparseRC achieves the best SHD and runtime in most scenarios, often even recovering the true DAG. GOLEM is significantly slower than SparseRC.

Varsortability. In Table 1 we also include the varsortability for each experimental setting. Our measurements for Erdős-Renyi graphs (all rows except row 2) are typically 1 – 5% lower than the measurements reported in [Reisach et al., 2021, Appendix G.1] for linear SEMs, but still high in general. However, the trivial variance-sorting method sortnregress fails overall. Note again that for fixed sparsity support (last row), all the methods fail and varsortability is lower. Therefore, in this scenario our data generating process poses a hard problem for DAG learning.

Experiment 2: Varying number of nodes or samples. In this experiment we first benchmark SparseRC with varying number of nodes (and thus number of edges) in the ground truth DAG, while keeping the data samples in \mathbf{X} equal to $n = 1000$. Second, we vary the number of samples, while keeping the number of nodes fixed to $d = 100$. All other parameters are set to default. The results are shown as plots in Fig. 2 reporting SHD, SID, and the runtime.

When varying the number of nodes (upper row Fig. 2) SparseRC, GOLEM, and NOTEARS achieve very good performance whereas the other methods perform significantly worse. As the number of nodes increases, SparseRC performs best and GOLEM and NOTEARS are reasonably close in terms of SHD and SID. However, both are significantly slower than ours. When increasing the number of samples (lower row Fig. 2) the overall performances

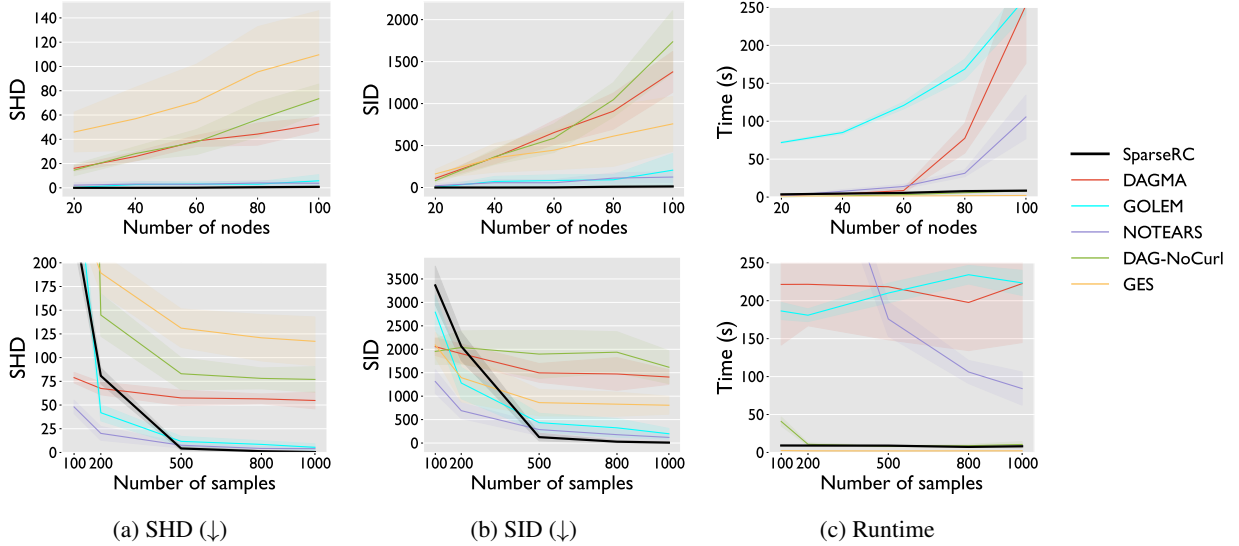


Figure 2: Plots illustrating SHD, SID and runtime (lower is better) on the default settings while varying the number of nodes with 1000 samples (first row) and varying the number of samples with 100 nodes (second row). The number of edges is twice the number of nodes in each case.

Table 3: Performance on larger DAGs.

Nodes d , samples n	SHD \downarrow			Runtime (s)		
	SparseRC	NOTEARS	GOLEM	SparseRC	NOTEARS	GOLEM
$d = 200, n = 500$	0	171	76	17.5	159.4	654.4
$d = 500, n = 1000$	0	377	114	123.6	467.9	6000.9
$d = 1000, n = 5000$	0	639	44	611.8	1550.7	39392.2
$d = 2000, n = 10000$	0	171	time-out	3932.7	8695.6	time-out
$d = 3000, n = 10000$	0	1904	time-out	12619.6	36180.0	time-out

(a) SHD \downarrow

(b) Runtime (s)

improve. For low number of samples SparseRC, GOLEM and NOTEARS fail. Their performance significantly improves after 500 samples where SparseRC overall achieves the best result. The rest of the methods have worse performance. SparseRC is again significantly faster than GOLEM and NOTEARS in this case.

Experiment 3: Larger DAGs. In our last experiment, shown in Table 3, we investigate the scalability of the best methods SparseRC, GOLEM, and NOTEARS from the previous experiments. We consider five different settings up to $d = 3000$ and $n = 10000$ samples. We use the prior default settings except for the sparsity of the root causes, which is now set to 5%. The metrics here are SHD and the runtime⁴. The results show that SparseRC excels in the very sparse setting with perfect reconstruction, far outperforming the others including in runtime. Moreover, SparseRC even recovers the edge weights with an average absolute error of about 1% for each case in Table 3.

5.2 Evaluation on a real dataset

Finally, we apply SparseRC on the causal protein-signaling network data provided by [Sachs et al., 2005]. The dataset consists of 7466⁵ samples from a network with 11 nodes that represent proteins and 17 edges showing the interaction between them. Even though this network is relatively small, the task of learning it is considered difficult and has been a common prior benchmark Ng et al. [2020], Gao et al. [2021], Yu et al. [2019], Zheng et al. [2018]. It is not known whether the assumption of few root causes holds in this case. We report the performance metrics for the most successful methods in Table 4.

⁴SID is computationally too expensive for a large number of nodes.

⁵As Lachapelle et al. [2019] we only use the first 853 samples. Differences may occur between the reported results and the literature due to different choice of hyperparameters and the use of 853 samples, where others might utilize the full dataset.

Table 4: Performance on the dataset from [Sachs et al., 2005].

	SHD ↓	SID ↓	NNZ
SparseRC	15	45	16
DAGMA	14	46	11
NOTEARS	11	44	15
GOLEM	21	43	19

The best SID is achieved by GOLEM (equal variance), which, however, has higher SHD. NOTEARS has the best SHD equal to 11. Overall, SparseRC performs well, achieving the closest number of edges to the real one with 16 and a competitive SHD and SID.

6 Broader Impact and Limitations

Our method inherits the broader impact of prior DAG learning methods including the important caveat for practical use that the learned DAG may not represent causal relations, whose discovery requires interventions. Further limitations that we share with prior work include (a) Learning DAGs beyond 10000 nodes are out of reach, (b) there is no theoretical convergence guarantee for the case that includes noise, (c) empirically, the performance drops in low varsortability, (d) our method is designed for linear SEMs like most of the considered benchmarks.

A specific limitation of our contribution is that it works well only for few root causes of varying location in the dataset.

7 Conclusion

We presented a new perspective on linear SEMs by introducing the notion of root causes. Mathematically, this perspective translates (or solves) the recurrence describing the SEM into an invertible linear transformation that takes as input DAG data, which we called root causes, to produce the observed data as output. Prior data generation for linear SEMs assumed a dense, random valued input vector. In this paper we motivated and studied the novel scenario of data generation and DAG learning for few root causes, i.e., a sparse input with noise, and noise in the measurement data. Our solution in this setting performs significantly better than prior algorithms, in particular for high sparsity where it can even recover the edge weights, is scalable to thousands of nodes, and thus expands the set of DAGs that can be learned in real-world scenarios where current methods fail.

References

- A. Amrollahi, A. Zandieh, M. Kapralov, and A. Krause. Efficiently learning Fourier sparse set functions. *Advances in Neural Information Processing Systems*, 32, 2019.
- B. Aragam and Q. Zhou. Concave penalized estimation of sparse gaussian bayesian networks. *The Journal of Machine Learning Research*, 16(1):2273–2328, 2015.
- K. Bello, B. Aragam, and P. Ravikumar. DAGMA: Learning DAGs via M-matrices and a Log-Determinant Acyclicity Characterization. *arXiv preprint arXiv:2209.08037*, 2022.
- P. Bühlmann, J. Peters, and J. Ernest. CAM: Causal additive models, high-dimensional order search and penalized regression. *The Annals of Statistics*, 42(6):2526–2556, 2014.
- B. Charpentier, S. Kibler, and S. Günnemann. Differentiable DAG Sampling. In *International Conference on Learning Representations*, 2022.
- M. Chevalley, Y. Roohani, A. Mehrjou, J. Leskovec, and P. Schwab. Causalbench: A large-scale benchmark for network inference from single-cell perturbation data. *arXiv preprint arXiv:2210.17283*, 2022.
- D. M. Chickering. Optimal structure identification with greedy search. *Journal of machine learning research*, 3(Nov):507–554, 2002.
- M. Chickering, D. Heckerman, and C. Meek. Large-sample learning of Bayesian networks is NP-hard. *Journal of Machine Learning Research*, 5:1287–1330, 2004.
- H. Cramér. Über eine eigenschaft der normalen verteilungsfunktion. *Mathematische Zeitschrift*, 41(1):405–414, 1936.
- Y. Gao, L. Shen, and S.-T. Xia. DAG-GAN: Causal structure learning with generative adversarial nets. In *ICASSP 2021-2021 IEEE International Conference on Acoustics, Speech and Signal Processing (ICASSP)*, pages 3320–3324. IEEE, 2021.
- A. Ghoshal and J. Honorio. Learning identifiable Gaussian Bayesian networks in polynomial time and sample complexity. *Advances in Neural Information Processing Systems*, 30, 2017.

- H. Hassanieh. *The Sparse Fourier Transform: Theory and Practice*, volume 19. Association for Computing Machinery and Morgan and Claypool, 2018.
- M. Kaiser and M. Sipos. Unsuitability of NOTEARS for Causal Graph Discovery when Dealing with Dimensional Quantities. *Neural Processing Letters*, pages 1–9, 2022.
- D. Kalainathan and O. Goudet. Causal discovery toolbox: Uncover causal relationships in python. *arXiv preprint arXiv:1903.02278*, 2019. URL <https://github.com/FenTechSolutions/CausalDiscoveryToolbox>.
- D. P. Kingma and J. Ba. Adam: A method for stochastic optimization. *arXiv preprint arXiv:1412.6980*, 2014.
- S. Lachapelle, P. Brouillard, T. Deleu, and S. Lacoste-Julien. Gradient-based neural dag learning. *arXiv preprint arXiv:1906.02226*, 2019.
- H.-C. Lee, M. Danieletto, R. Miotto, S. T. Cherng, and J. T. Dudley. Scaling structural learning with NO-BEARS to infer causal transcriptome networks. In *PACIFIC SYMPOSIUM ON BIOCOMPUTING 2020*, pages 391–402. World Scientific, 2019.
- D. J. Lehmann. Algebraic structures for transitive closure. *Theoretical Computer Science*, 4(1):59–76, 1977.
- P. Lévy. Propriétés asymptotiques des sommes de variables aléatoires enchaînées. *Bull. Sci. Math*, 59(84-96):109–128, 1935.
- P.-L. Loh and P. Bühlmann. High-dimensional learning of linear causal networks via inverse covariance estimation. *The Journal of Machine Learning Research*, 15(1):3065–3105, 2014.
- I. Ng, A. Ghassami, and K. Zhang. On the role of sparsity and dag constraints for learning linear dags. *Advances in Neural Information Processing Systems*, 33:17943–17954, 2020.
- R. Pamfil, N. Sriwattanaworachai, S. Desai, P. Pilgerstorfer, K. Georgatzis, P. Beaumont, and B. Aragam. Dynotears: Structure learning from time-series data. In *International Conference on Artificial Intelligence and Statistics*, pages 1595–1605. PMLR, 2020.
- J. Peters and P. Bühlmann. Identifiability of Gaussian structural equation models with equal error variances. *Biometrika*, 101(1): 219–228, 2014.
- J. Peters and P. Bühlmann. Structural intervention distance for evaluating causal graphs. *Neural computation*, 27(3):771–799, 2015.
- J. Peters, D. Janzing, and B. Schölkopf. *Elements of causal inference: foundations and learning algorithms*. The MIT Press, 2017.
- C. Ramirez, V. Kreinovich, and M. Argaez. Why ℓ_1 is a good approximation to ℓ_0 : A Geometric Explanation. *Journal of Uncertain Systems*, 7(3):203–207, 2013.
- J. Ramsey, M. Glymour, R. Sanchez-Romero, and C. Glymour. A million variables and more: the fast greedy equivalence search algorithm for learning high-dimensional graphical causal models, with an application to functional magnetic resonance images. *International journal of data science and analytics*, 3(2):121–129, 2017.
- A. Reisach, C. Seiler, and S. Weichwald. Beware of the simulated dag! causal discovery benchmarks may be easy to game. *Advances in Neural Information Processing Systems*, 34:27772–27784, 2021.
- K. Sachs, O. Perez, D. Pe’er, D. A. Lauffenburger, and G. P. Nolan. Causal protein-signaling networks derived from multiparameter single-cell data. *Science*, 308(5721):523–529, 2005.
- B. Seifert, C. Wendler, and M. Püschel. Causal Fourier Analysis on Directed Acyclic Graphs and Posets. *arXiv preprint arXiv:2209.07970*, 2022a.
- B. Seifert, C. Wendler, and M. Püschel. Learning Fourier-Sparse Functions on DAGs. In *ICLR2022 Workshop on the Elements of Reasoning: Objects, Structure and Causality*, 2022b.
- S. Shimizu, P. O. Hoyer, A. Hyvärinen, and A. Kerminen. A Linear Non-Gaussian Acyclic Model for Causal Discovery. *Journal of Machine Learning Research*, 7(72):2003–2030, 2006. URL <http://jmlr.org/papers/v7/shimizu06a.html>.
- P. Stobbe and A. Krause. Learning Fourier sparse set functions. In *Artificial Intelligence and Statistics*, pages 1125–1133. PMLR, 2012.
- I. Tsamardinos, L. E. Brown, and C. F. Aliferis. The max-min hill-climbing Bayesian network structure learning algorithm. *Machine learning*, 65(1):31–78, 2006.
- M. J. Vowels, N. C. Camgoz, and R. Bowden. D’ya like DAGs? A survey on structure learning and causal discovery. *ACM Computing Surveys (CSUR)*, 2021.
- Y. Yu, J. Chen, T. Gao, and M. Yu. DAG-GNN: DAG structure learning with graph neural networks. In *International Conference on Machine Learning*, pages 7154–7163. PMLR, 2019.
- Y. Yu, T. Gao, N. Yin, and Q. Ji. DAGs with no curl: An efficient DAG structure learning approach. In *International Conference on Machine Learning*, pages 12156–12166. PMLR, 2021.
- V. Zantedeschi, J. Kaddour, L. Franceschi, M. Kusner, and V. Niculae. DAG Learning on the Permutahedron. In *ICLR2022 Workshop on the Elements of Reasoning: Objects, Structure and Causality*, 2022.
- X. Zheng, B. Aragam, P. K. Ravikumar, and E. P. Xing. Dags with no tears: Continuous optimization for structure learning. *Advances in Neural Information Processing Systems*, 31, 2018.
- X. Zheng, C. Dan, B. Aragam, P. Ravikumar, and E. Xing. Learning sparse nonparametric dags. In *International Conference on Artificial Intelligence and Statistics*, pages 3414–3425. PMLR, 2020.

A Additional experimental results

Experiment 1: Different application scenarios. We present additional experimental results to include more metrics and baselines. The results support our observations and conclusions from the main text. First, we expand Table 1 of the main text reporting the SHD metric and provide the computation of SHD, TPR and SID in the tables below. Those further include the methods LiNGAM [Shimizu et al., 2006], fGES [Ramsey et al., 2017], MMHC [Tsamardinos et al., 2006] and CAM [Bühlmann et al., 2014].

Table 5: SHD (lower is better) for learning DAGs with 40 nodes and 80 edges. Each row is an experiment. The first row is the default, whose settings are in the blue column. In each other row, exactly one default parameter is changed (change). The last six columns correspond to prior algorithms. The best results are shown bold. Entries with SHD higher than 80 are reported as *failure*.

(a)

Hyperparameter	Default value	Current value	SparseRC (ours)	DAGMA	GOLEM	NOTEARS	DAG-NoCurl
1. Default settings			0.00 ± 0.00	25.80 ± 3.71	2.70 ± 2.24	3.10 ± 2.30	28.20 ± 5.67
2. Graph type	Erdős-Renyi	Scale-free	0.00 ± 0.00	26.20 ± 4.79	1.10 ± 1.38	0.90 ± 0.94	7.60 ± 5.68
3. Edges / Vertices	2	3	0.90 ± 1.04	44.40 ± 7.10	4.30 ± 2.87	10.40 ± 8.26	40.50 ± 14.02
4. Larger weights in A	(0.4, 0.8)	(0.5, 2)	23.10 ± 13.66	13.80 ± 3.63	1.60 ± 3.26	8.50 ± 8.42	20.30 ± 8.53
5. High sparsity in C	$p = 0.3$	$p = 0.1$	0.00 ± 0.00	65.70 ± 3.23	4.90 ± 4.28	9.80 ± 2.31	36.90 ± 7.78
6. Low sparsity in C	$p = 0.3$	$p = 0.6$	64.80 ± 4.40	14.30 ± 4.22	2.50 ± 1.96	2.50 ± 1.36	32.30 ± 11.44
7. N_c, N_x deviation	$\sigma = 0.01$	$\sigma = 0.1$	3.50 ± 1.75	21.00 ± 2.53	2.50 ± 1.36	3.50 ± 2.50	26.40 ± 8.91
8. N_c, N_x distribution	Gaussian	Gumbel	0.20 ± 0.40	27.00 ± 3.29	4.10 ± 2.98	4.60 ± 3.38	24.30 ± 8.06
9. Measurement noise	$N_c \neq 0, N_x = 0$	$N_c = 0, N_x \neq 0$	0.10 ± 0.30	24.10 ± 3.70	3.40 ± 4.15	2.80 ± 1.72	30.10 ± 9.54
10. Full Noise	$N_c \neq 0, N_x = 0$	$N_c \neq 0, N_x \neq 0$	0.30 ± 0.64	27.50 ± 3.17	2.10 ± 1.51	4.00 ± 3.71	31.70 ± 8.15
11. Standardization	No	Yes	78.70 ± 3.93	62.70 ± 7.40	67.70 ± 8.99	79.60 ± 6.84	failure
12. Samples	n=1000	n = 20	failure	76.10 ± 4.72	failure	failure	failure
13. Fixed support	No	Yes	failure	73.50 ± 4.18	failure	failure	failure

(b)

Hyperparameter	Default value	Current value	GES	sortnregress	LiNGAM	fGES	MMHC	CAM
1. Default settings			56.90 ± 25.84	failure	failure	failure	failure	failure
2. Graph type	Erdős-Renyi	Scale-free	78.00 ± 39.52	33.30 ± 9.23	failure	failure	failure	failure
3. Edges / Vertices	2	3	failure	failure	failure	failure	failure	failure
4. Larger weights in A	(0.4, 0.8)	(0.5, 2)	64.30 ± 35.96	failure	failure	failure	failure	failure
5. High sparsity in C	$p = 0.3$	$p = 0.1$	47.40 ± 25.42	failure	failure	failure	failure	failure
6. Low sparsity in C	$p = 0.3$	$p = 0.6$	63.60 ± 25.05	failure	failure	failure	failure	66.00 ± 9.53
7. N_c, N_x deviation	$\sigma = 0.01$	$\sigma = 0.1$	50.80 ± 13.37	75.40 ± 19.27	failure	failure	failure	failure
8. N_c, N_x distribution	Gaussian	Gumbel	53.10 ± 21.19	failure	failure	failure	failure	failure
9. Measurement noise	$N_c \neq 0, N_x = 0$	$N_c = 0, N_x \neq 0$	54.10 ± 18.25	failure	failure	failure	failure	failure
10. Full Noise	$N_c \neq 0, N_x = 0$	$N_c \neq 0, N_x \neq 0$	69.10 ± 29.90	failure	failure	failure	failure	failure
11. Standardization	No	Yes	41.80 ± 17.97	failure	failure	failure	failure	79.70 ± 12.91
12. Samples	n=1000	n = 20	failure	error	error	error	failure	time-out
13. Fixed support	No	Yes	56.10 ± 8.25	failure	failure	75.40 ± 9.24	failure	76.50 ± 5.41

Table 6: TPR (higher is better). Entries with TPR lower than 0.5 are reported as *failure*.

(a)

Hyperparameter	Default value	Current value	SparseRC (ours)	DAGMA	GOLEM	NOTEARS	DAG-NoCurl
1. Default settings			1.00 ± 0.00	0.68 ± 0.05	0.97 ± 0.03	0.96 ± 0.03	0.83 ± 0.04
2. Graph type	Erdős-Renyi	Scale-free	1.00 ± 0.00	0.66 ± 0.06	0.99 ± 0.01	0.99 ± 0.01	0.97 ± 0.02
3. Edges / Vertices	2	3	0.99 ± 0.01	0.63 ± 0.05	0.97 ± 0.02	0.95 ± 0.04	0.84 ± 0.06
4. Larger weights in A	(0.4, 0.8)	(0.5, 2)	0.88 ± 0.07	0.85 ± 0.04	0.99 ± 0.02	0.94 ± 0.05	0.94 ± 0.02
5. High sparsity in C	$p = 0.3$	$p = 0.1$	1.00 ± 0.00	failure	0.95 ± 0.03	0.88 ± 0.03	0.78 ± 0.06
6. Low sparsity in C	$p = 0.3$	$p = 0.6$	failure	0.82 ± 0.05	0.97 ± 0.02	0.97 ± 0.02	0.81 ± 0.04
7. N_c, N_x deviation	$\sigma = 0.01$	$\sigma = 0.1$	0.96 ± 0.02	0.74 ± 0.03	0.97 ± 0.01	0.96 ± 0.03	0.83 ± 0.06
8. N_c, N_x distribution	Gaussian	Gumbel	1.00 ± 0.01	0.66 ± 0.04	0.96 ± 0.03	0.95 ± 0.03	0.86 ± 0.04
9. Measurement noise	$N_c \neq 0,$ $N_x = 0$	$N_c = 0,$ $N_x \neq 0$	1.00 ± 0.00	0.70 ± 0.05	0.96 ± 0.05	0.97 ± 0.02	0.81 ± 0.05
10. Full Noise	$N_c \neq 0,$ $N_x = 0$	$N_c \neq 0,$ $N_x \neq 0$	1.00 ± 0.01	0.66 ± 0.04	0.97 ± 0.02	0.95 ± 0.04	0.81 ± 0.04
11. Standardization	No	Yes	failure	failure	failure	failure	failure
12. Samples	n=1000	$n = 20$	failure	failure	failure	failure	failure
13. Fixed support	No	Yes	failure	failure	failure	failure	0.54 ± 0.08

(b)

Hyperparameter	Default value	Current value	GES	sortnregress	LiNGAM	fGES	MMHC	CAM
1. Default settings			0.82 ± 0.10	0.93 ± 0.02	failure	0.88 ± 0.05	0.89 ± 0.02	failure
2. Graph type	Erdős-Renyi	Scale-free	0.88 ± 0.09	0.98 ± 0.02	failure	0.82 ± 0.07	0.76 ± 0.04	failure
3. Edges / Vertices	2	3	0.66 ± 0.10	0.92 ± 0.03	failure	0.81 ± 0.06	0.66 ± 0.06	0.52 ± 0.05
4. Larger weights in A	(0.4, 0.8)	(0.5, 2)	0.82 ± 0.09	0.95 ± 0.03	failure	0.85 ± 0.08	0.55 ± 0.07	failure
5. High sparsity in C	$p = 0.3$	$p = 0.1$	0.85 ± 0.07	0.90 ± 0.02	failure	0.84 ± 0.07	0.86 ± 0.04	failure
6. Low sparsity in C	$p = 0.3$	$p = 0.6$	0.78 ± 0.09	0.90 ± 0.03	failure	0.86 ± 0.07	0.89 ± 0.02	0.55 ± 0.06
7. N_c, N_x deviation	$\sigma = 0.01$	$\sigma = 0.1$	0.81 ± 0.08	0.92 ± 0.03	failure	0.84 ± 0.06	0.87 ± 0.06	failure
8. N_c, N_x distribution	Gaussian	Gumbel	0.85 ± 0.05	0.91 ± 0.03	failure	0.88 ± 0.03	0.88 ± 0.06	failure
9. Measurement noise	$N_c \neq 0,$ $N_x = 0$	$N_c = 0,$ $N_x \neq 0$	0.82 ± 0.06	0.91 ± 0.04	failure	0.84 ± 0.06	0.89 ± 0.02	failure
10. Full Noise	$N_c \neq 0,$ $N_x = 0$	$N_c \neq 0,$ $N_x \neq 0$	0.79 ± 0.07	0.90 ± 0.03	failure	0.88 ± 0.06	0.86 ± 0.04	failure
11. Standardization	No	Yes	0.88 ± 0.06	0.51 ± 0.06	0.53 ± 0.08	0.87 ± 0.07	0.88 ± 0.04	failure
12. Samples	n=1000	$n = 20$	failure	error	error	error	failure	time-out
13. Fixed support	No	Yes	0.66 ± 0.08	failure	failure	0.52 ± 0.08	failure	failure

Table 7: SID (lower is better).

(a)

Hyperparameter	Default value	Current value	SparseRC (ours)	DAGMA	GOLEM	NOTEARS	DAG-NoCurl
1. Default settings			0.00 ± 0.00	360.10 ± 76.42	72.50 ± 60.23	57.60 ± 36.73	366.90 ± 92.16
2. Graph type	Erdős-Renyi	Scale-free	0.00 ± 0.00	108.90 ± 21.27	9.40 ± 11.23	7.60 ± 10.17	30.90 ± 26.82
3. Edges / Vertices	2	3	22.70 ± 31.61	684.80 ± 124.98	117.00 ± 80.48	208.10 ± 138.95	506.00 ± 129.90
4. Larger weights in A	(0.4, 0.8)	(0.5, 2)	163.20 ± 96.06	215.10 ± 41.66	19.00 ± 31.59	91.50 ± 85.16	74.20 ± 39.79
5. High sparsity in C	$p = 0.3$	$p = 0.1$	0.00 ± 0.00	767.10 ± 70.99	94.50 ± 74.59	155.70 ± 60.87	396.50 ± 92.94
6. Low sparsity in C	$p = 0.3$	$p = 0.6$	768.00 ± 113.93	177.80 ± 49.36	56.50 ± 52.95	45.80 ± 23.45	349.60 ± 52.37
7. N_c, N_x deviation	$\sigma = 0.01$	$\sigma = 0.1$	66.70 ± 42.98	316.80 ± 50.24	62.30 ± 48.84	78.80 ± 54.34	323.60 ± 104.48
8. N_c, N_x distribution	Gaussian	Gumbel	4.00 ± 8.20	392.10 ± 63.01	71.50 ± 44.83	74.80 ± 47.63	309.30 ± 68.31
9. Measurement noise	$N_c \neq 0, N_x = 0$	$N_c = 0, N_x \neq 0$	2.30 ± 6.90	355.30 ± 55.09	66.20 ± 72.59	51.80 ± 31.57	376.20 ± 135.27
10. Full Noise	$N_c \neq 0, N_x = 0$	$N_c \neq 0, N_x \neq 0$	5.20 ± 10.41	417.00 ± 117.40	52.80 ± 30.52	86.20 ± 86.94	359.70 ± 63.59
11. Standardization	No	Yes	1051.10 ± 55.95	984.40 ± 93.02	1042.70 ± 83.01	1060.10 ± 104.50	1223.90 ± 55.85
12. Samples	$n=1000$	$n = 20$	697.10 ± 71.45	734.30 ± 65.36	696.70 ± 115.66	746.70 ± 64.93	507.60 ± 86.62
13. Fixed support	No	Yes	734.10 ± 146.96	828.60 ± 83.57	921.90 ± 94.42	845.10 ± 58.60	539.10 ± 152.46

(b)

Hyperparameter	Default value	Current value	GES	sortnregress	LiNGAM	fGES	MMHC	CAM
1. Default settings			353.60 ± 170.24	81.60 ± 79.40	960.90 ± 144.11	610.80 ± 95.19	SID time-out	884.10 ± 110.13
2. Graph type	Erdős-Renyi	Scale-free	100.30 ± 56.10	9.70 ± 7.94	1047.10 ± 230.94	221.70 ± 58.73	SID time-out	773.10 ± 80.52
3. Edges / Vertices	2	3	818.90 ± 177.78	245.10 ± 75.82	1145.80 ± 53.54	1113.30 ± 133.30	SID time-out	1168.80 ± 57.31
4. Larger weights in A	(0.4, 0.8)	(0.5, 2)	356.70 ± 120.32	61.00 ± 49.13	1327.10 ± 71.14	548.90 ± 63.24	SID time-out	786.00 ± 132.55
5. High sparsity in C	$p = 0.3$	$p = 0.1$	315.10 ± 102.08	122.40 ± 58.20	1336.50 ± 40.15	682.20 ± 93.76	SID time-out	990.90 ± 122.69
6. Low sparsity in C	$p = 0.3$	$p = 0.6$	397.10 ± 162.91	100.70 ± 26.81	1214.10 ± 200.08	715.10 ± 213.44	SID time-out	800.50 ± 132.00
7. N_c, N_x deviation	$\sigma = 0.01$	$\sigma = 0.1$	374.60 ± 124.97	138.00 ± 85.32	1015.00 ± 160.63	710.10 ± 135.50	SID time-out	951.70 ± 123.78
8. N_c, N_x distribution	Gaussian	Gumbel	305.00 ± 99.13	118.20 ± 57.53	978.60 ± 117.06	638.30 ± 99.88	SID time-out	878.70 ± 170.31
9. Measurement noise	$N_c \neq 0, N_x = 0$	$N_c = 0, N_x \neq 0$	374.90 ± 138.53	135.70 ± 61.93	994.00 ± 141.81	753.60 ± 100.26	SID time-out	973.70 ± 136.36
10. Full Noise	$N_c \neq 0, N_x = 0$	$N_c \neq 0, N_x \neq 0$	422.00 ± 158.70	153.60 ± 84.11	972.10 ± 78.94	659.10 ± 151.38	SID time-out	878.20 ± 170.19
11. Standardization	No	Yes	270.20 ± 108.67	871.10 ± 72.21	823.80 ± 170.36	726.20 ± 134.10	SID time-out	908.70 ± 153.04
12. Samples	$n=1000$	$n = 20$	802.30 ± 112.75	error	error	error	SID time-out	time-out
13. Fixed support	No	Yes	479.10 ± 71.45	589.10 ± 132.59	1080.00 ± 54.93	699.10 ± 124.86	SID time-out	701.30 ± 82.67

Experiment 2: Varying number of nodes or samples. In addition to Fig. 2 we include the plots of Fig. 3 for the experiments that vary the number of nodes of the ground truth DAG or the number of samples in the data. The plots include the methods LiNGAM, fGES, MMHC and CAM and additionally contain the metrics TPR, NNZ regarding the unweighted adjacency matrix and NMSE with respect to the weighted approximation of the adjacency matrix.

Experiment 3: Larger DAGs. In our last experiment our method achieved perfect reconstruction, so we further investigate whether the true weights were recovered. Table 8 reports metrics that evaluate the weighted approximation of the true adjacency matrix.

We compute the average L^1 loss $\frac{\|\mathbf{A} - \hat{\mathbf{A}}\|_1}{|E|}$, the Max- L^1 loss $\max_{i,j} |\mathbf{A}_{ij} - \hat{\mathbf{A}}_{ij}|$, the average L^2 loss $\frac{\|\mathbf{A} - \hat{\mathbf{A}}\|_2}{|E|}$ and the NMSE $\frac{\|\mathbf{A} - \hat{\mathbf{A}}\|_2}{\|\mathbf{A}\|_2}$.

Table 8: SparseRC weight reconstruction performance on larger DAGs.

Nodes d , samples n	Avg. L^1 loss	Max- L^1 loss	Avg. L^2 loss	NMSE
$d = 200, n = 500$	0.012	0.050	0.001	0.026
$d = 500, n = 1000$	0.012	0.084	0.000	0.025
$d = 1000, n = 5000$	0.010	0.223	0.000	0.023
$d = 2000, n = 10000$	0.010	0.266	0.000	0.023
$d = 3000, n = 10000$	0.011	0.344	0.000	0.025

A.1 Implementation details

Training details. In the implementation of SparseRC we initiate a PyTorch nn.Module with a single $d \times d$ weighted matrix represented as a linear layer. The model is trained so that the final result will have a weight matrix which approximates the original DAG adjacency matrix. To train our model we use the Adam optimizer [Kingma and Ba, 2014] with learning rate 10^{-3} . Moreover, note that we do not use the L^1 regularizer of the adjacency matrix as NOTEARS, so the λ parameter of optimization problem (9) is

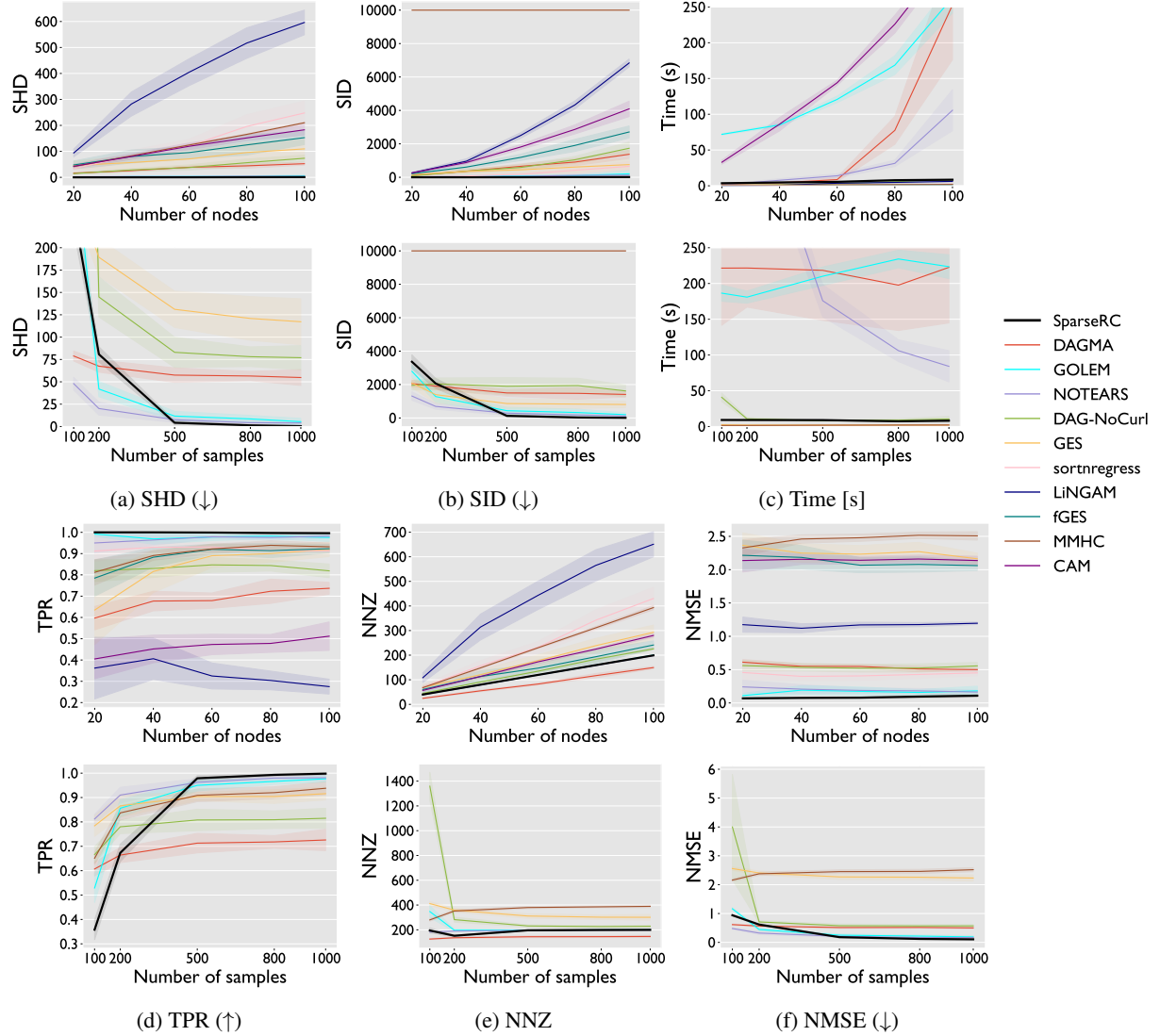


Figure 3: Plots illustrating performance metrics (a) SHD (lower is better), (b) SID (lower is better), (c) Time [seconds], (d) TPR (higher is better), (e) NNZ and (f) NMSE (lower is better). Each metric is evaluated in two experimental scenarios: when varying the number of rows (upper figure) and when varying the number of samples (lower figure).

$\lambda = 0$ in our case. For NOTEARS we choose $\lambda = 5 \cdot 10^{-3}$ and $\lambda = 10^{-3}$ for the case of more dense graphs (Edges/Vertices = 3, row 3). For the rest of the baselines we choose default hyperparameters.

Resources. Our experiments were run on a single laptop machine with 8 core CPU with 32GB RAM and an NVIDIA GeForce RTX 3080 GPU.

Licenses. We use code repositories that are open-source and publicly available on github. All repositories licensed under the Apache 2.0 or MIT license. In particular we use the github repositories of DAGMA [Bello et al., 2022] <https://github.com/kevinsbello/dagma>, GOLEM [Ng et al., 2020] <https://github.com/ignavierng/golem>, NOTEARS [Zheng et al., 2018] <https://github.com/xunzheng/notears>, DAG-NoCurl [Yu et al., 2021] <https://github.com/fishmoon1234/DAG-NoCurl>, LiNGAM [Shimizu et al., 2006] <https://github.com/cdt15/lingam> and the causal discovery toolbox [Kalainathan and Goudet, 2019] <https://github.com/FenTechSolutions/CausalDiscoveryToolbox>. Our code is licensed under the MIT license and will be released in public.

B Global Minimizer

We provide the proof of Theorem 3.2 of the main paper. The data \mathbf{X} are assumed to be generated via noise-less root causes as described in the main paper. We denote by $\hat{\mathbf{A}}$ the optimal solution of the optimization problem (8). In particular what we will show the following result, from which our theorem follows directly.

Theorem B.1. *Consider a DAG with weighted adjacency matrix \mathbf{A} . Given that the number of data n satisfies*

$$n \geq \frac{2^{3d-2}d(d-1)}{(1-\delta)^2 p^k (1-p)^{d-k}} \quad (11)$$

where $k = \lfloor dp \rfloor$ and

$$\delta \geq \max \left\{ \frac{1}{p^k (1-p)^{d-k} \binom{d}{k}} \sqrt{\frac{1}{2} \ln \left(\frac{1}{\epsilon} \right)}, \binom{d}{k} \sqrt{\frac{1}{2} \ln \left(\frac{\binom{d}{k}}{\epsilon} \right)} \right\}. \quad (12)$$

Then with probability $(1-\epsilon)^2$ the solution to the optimization problem (8) coincides with the true DAG, namely $\hat{\mathbf{A}} = \mathbf{A}$.

Remark B.2. The reason we choose $k = \lfloor dp \rfloor$ is that because of the Bernoulli trials for the non-zero root causes, the expected value of the cardinality of the support will be exactly $\lfloor dp \rfloor$. Thus we expect to have more concentration on that value of k which is something we desire, since in the proof we use all possible patterns with support equal to k .

We begin the proof with some important observations and definitions.

Lemma B.3. *If $\widehat{\mathbf{A}} = \overline{\mathbf{A}}$ then $\hat{\mathbf{A}} = \mathbf{A}$.*

Proof. We have that

$$\mathbf{I} + \widehat{\mathbf{A}} = \mathbf{I} + \overline{\mathbf{A}} \Leftrightarrow (\mathbf{I} + \widehat{\mathbf{A}})^{-1} = (\mathbf{I} + \overline{\mathbf{A}})^{-1} \Leftrightarrow (\mathbf{I} - \hat{\mathbf{A}}) = (\mathbf{I} - \mathbf{A}) \Leftrightarrow \hat{\mathbf{A}} = \mathbf{A} \quad (13)$$

□

Definition B.4. We define $\hat{\mathbf{C}} = \mathbf{X} - \mathbf{X}\hat{\mathbf{A}}$ the root causes corresponding to the optimal adjacency matrix.

Definition B.5. Let $S \subset \{1, 2, 3, \dots, d\}$ be a set of indices. We say that a root causes vector \mathbf{c} has support S if $c_i = 0$ for $i \in [d] \setminus S$.

Definition B.6. For a given support S we consider the set $R \subset [n]$ of the rows of \mathbf{C} that have support S . Then, $\mathbf{C}_R, \hat{\mathbf{C}}_R$ denote the submatrices consisting of the rows with indices in R .

Lemma B.7. *For any row subset $R \subset [n]$ we have that $\text{rank}(\hat{\mathbf{C}}_R) = \text{rank}(\mathbf{C}_R)$*

Proof. We have that

$$\hat{\mathbf{C}}(\mathbf{I} + \widehat{\mathbf{A}}) = \mathbf{X} = \mathbf{C}(\mathbf{I} + \overline{\mathbf{A}}) \quad (14)$$

Therefore, since both $\mathbf{A}, \hat{\mathbf{A}}$ are acyclic and $\mathbf{I} + \widehat{\mathbf{A}}, \mathbf{I} + \overline{\mathbf{A}}$ are invertible we have that

$$\hat{\mathbf{C}}_R(\mathbf{I} + \widehat{\mathbf{A}}) = \mathbf{C}_R(\mathbf{I} + \overline{\mathbf{A}}) \Leftrightarrow \text{rank}(\hat{\mathbf{C}}_R) = \text{rank}(\mathbf{C}_R) \quad (15)$$

□

Lemma B.8. *For any row subset $R \subset [n]$ of root causes \mathbf{C} with the same support S such that $|S| = k$ and $|R| = r \geq k$ the nonzero columns of \mathbf{C}_R are linearly independent with probability 1 and therefore $\text{rank}(\mathbf{C}_R) = k$.*

Proof. assume $\mathbf{c}_1, \dots, \mathbf{c}_k$ are the non-zero columns of \mathbf{C}_R . Then each \mathbf{c}_i is a vector of dimension r whose each entry is sampled uniformly at random in the range $[0.5, 1]$. Given any $k-1$ vectors from $\mathbf{c}_1, \dots, \mathbf{c}_k$ their linear span can at most make a subspace of $[0.5, 1]^r$ of dimension at most $k-1$. However, since every \mathbf{c}_i is sampled uniformly at random from $[0.5, 1]^r$ and $r \geq k > k-1$ the probability that \mathbf{c}_i lies in the linear span of the other $k-1$ vectors has measure 0. Therefore, the required result holds with probability 1. □

Lemma B.9. *With probability $(1-\epsilon)^2$ for every different support S with $|S| = k$ there are rows R such that \mathbf{C}_R have support S and*

$$|R| > 2^{3d-2}d(d-1) \quad (16)$$

Proof. Set $l = 2^{3d-2}d(d-1)$ and $K = \frac{l \binom{d}{k}}{(1-\delta)}$. Also set N be the random variable representing the number of root causes \mathbf{c} with $|\text{supp}(\mathbf{c})| = k$ and N_i the number of repetitions of the i -th k -support pattern, $i = 1, \dots, \binom{d}{k}$.

We first use conditional probability.

$$\mathbb{P}(N \geq K \cap N_i \geq l, \forall i) = \mathbb{P}(N_i \geq l, \forall i | N \geq K) \mathbb{P}(N \geq K) \quad (17)$$

Now we will show that $\mathbb{P}(N \geq K) \geq (1 - \epsilon)$ and $\mathbb{P}(N_i \geq l, \forall i | N \geq K) \geq (1 - \epsilon)$ using Chernoff bounds. From Hoeffding inequality we get:

$$\mathbb{P}(N \leq (1 - \delta)\mu) \leq e^{-2\delta^2\mu^2/n^2} \quad (18)$$

where $\mu = np^k(1-p)^{d-k} \binom{d}{k}$ is the expected value of N , $\delta \geq \frac{1}{p^k(1-p)^{d-k} \binom{d}{k}} \sqrt{\frac{1}{2} \ln \left(\frac{1}{\epsilon}\right)}$ and $n \geq \frac{1}{1-\delta} \frac{K}{p^k(1-p)^{d-k} \binom{d}{k}}$ so

$$\mathbb{P}(N \leq K) \leq \mathbb{P}(N \leq (1 - \delta)\mu) \leq e^{-2\delta^2\mu^2/n^2} \leq \epsilon \Leftrightarrow \mathbb{P}(N \geq K) \geq 1 - \epsilon \quad (19)$$

Now given that we have at least K root causes with support exactly k , we will show that, on exactly K such root causes, each different pattern will appear at least l times with probability $(1 - \epsilon)$. From the union bound

$$\mathbb{P}\left(\bigcup_i N_i \leq l\right) \leq \sum_i \mathbb{P}(N_i \leq l) \quad (20)$$

So we need to show that $\mathbb{P}(N_i \leq l) \leq \frac{\epsilon}{\binom{d}{k}}$. We use again the Hoeffding inequality.

$$\mathbb{P}(N_i \leq (1 - \delta)\mu) \leq e^{-2\delta^2\mu^2/K^2} \quad (21)$$

where the expected value is $\mu = \frac{K}{\binom{d}{k}} = \frac{l}{1-\delta}$ since now the probability is uniform over all possible k -sparsity patterns. Given

$\delta \geq \binom{d}{k} \sqrt{\frac{1}{2} \ln \left(\frac{\binom{d}{k}}{\epsilon}\right)}$ we derive

$$\mathbb{P}(N_i \leq l) = \mathbb{P}(N_i \leq (1 - \delta)\mu) \leq e^{-2\delta^2\mu^2/K^2} \leq \frac{\epsilon}{\binom{d}{k}} \quad (22)$$

The result follows. \square

Lemma B.10. Assume that the data number n is large enough so that for every different support S we have the rows R such that \mathbf{C}_R have support S and $|R| > 2^d l$ where

$$l > 2^{2d-2} d(d-1) = 2^d \sum_{k=2}^d \binom{d}{k} k(k-1) \quad (23)$$

Then there exist rows \hat{R} such that $|\hat{R}| > k$, $\mathbf{C}_{\hat{R}}$ has support S and $\hat{\mathbf{C}}_{\hat{R}}$ has support \hat{S} with $|\hat{S}| = k$. Moreover, both the non-zero columns of $\mathbf{C}_{\hat{R}}$, $\hat{\mathbf{C}}_{\hat{R}}$ form two linearly independent set of vectors. In words, this means that the data are many enough so we can always find pairs of corresponding submatrices of root causes with each consisting of k non-zero columns.

Proof. According to the assumption there exists a row-submatrix \mathbf{C}_R where all rows have support R and $|R| > 2^d l$. Group the root causes $\hat{\mathbf{C}}_R$ into all different supports, which are 2^d in number. Take any such group $R' \subset R$ of rows of $\hat{\mathbf{C}}$ that all have the same support S' . If $|R'| \geq k$ then from Lemma B.7 $\text{rank}(\hat{\mathbf{C}}_{R'}) = \text{rank}(\mathbf{C}_{R'}) = k$ so $\hat{\mathbf{C}}_{R'}$ will have at least k non-zero columns, and since the support is fixed, it will have at least k non-zero elements at each row, which means at least as many non-zeros as $\mathbf{C}_{R'}$. Therefore $\hat{\mathbf{C}}_{R'}$ can only have less non-zero elements if $|R'| < k$, and in that case $\mathbf{C}_{R'}$ has at most $k(k-1)$ more elements. If we count for all $k = 1, \dots, d$ all different supports of $\hat{\mathbf{C}}_{R'}$ for all possible supports of \mathbf{C}_R this gives that $\hat{\mathbf{C}}$ can have at most $\sum_{k=2}^d \binom{d}{k} 2^d k(k-1)$ less non-zero elements compared to \mathbf{C} .

Due to the pigeonhole principle, there exists $\hat{R} \subset R$ and $|\hat{R}| > l$ with $\hat{\mathbf{C}}_{\hat{R}}$ all having the same support \hat{S} , not necessarily equal to S . According to our previous explanation we need to have at least k non-zero columns in $\hat{\mathbf{C}}_{\hat{R}}$. If we had $k+1$ columns then this would give l more non-zero elements, but

$$l > 2^{2d-2} d(d-1) = 2^d d(d-1) 2^{d-2} = 2^d \sum_{k=0}^{d-2} \binom{d-2}{k-2} d(d-1) = 2^d \sum_{k=2}^d \binom{d}{k} k(k-1) \quad (24)$$

So then $\|\hat{\mathbf{C}}\|_0 > \|\mathbf{C}\|_0$ which is a contradiction due to the optimality of $\hat{\mathbf{A}}$. Therefore, $\hat{\mathbf{C}}_{\hat{R}}$ has exactly k non-zero columns which necessarily need to be linearly independent in order to have $\text{rank}(\hat{\mathbf{C}}_{\hat{R}}) = \text{rank}(\mathbf{C}_{\hat{R}}) = k$ as necessary. The linear independence of the columns of $\mathbf{C}_{\hat{R}}$ follows from Lemma B.8 since $l \gg k$. \square

Definition B.11. A pair $\mathbf{C}_R, \hat{\mathbf{C}}_R$ constructed according to Lemma B.10 that have fixed support S, \hat{S} respectively with cardinality k each and $|R|$ large enough so that $\text{rank}(\hat{\mathbf{C}}_{\hat{R}}) = \text{rank}(\mathbf{C}_{\hat{R}}) = k$, will be called a k -pair of submatrices.

Remark B.12. For notational simplicity we will drop the index R whenever the choice of the rows according to the sparsity pattern S is defined in the context.

The complete Theorem B.1 follows after combining the following two propositions.

Proposition B.13. *If the data \mathbf{X} are indexed such that \mathbf{A} is upper triangular, then so is $\widehat{\mathbf{A}}$.*

Remark B.14. Notice that \mathbf{A} is upper triangular if and only if $\overline{\mathbf{A}}$ is upper triangular. This holds as the polynomial $1+x+x^2+\dots+x^{d-2}$ doesn't have real roots. Thus we only need to show that $\overline{a}_{ji} = 0$ for all $i < j$.

Before we proceed to the proof of Prop. B.13 we first prove the following helpful lemma.

Lemma B.15. *Consider $\mathbf{C}, \widehat{\mathbf{C}}$ a k -pair. Also let \mathbf{X} be the corresponding submatrix of data. If $\mathbf{X}_{:,i} = \mathbf{0}$ then*

$$\widehat{\mathbf{C}}_{:,i} = \mathbf{0} \text{ and } \overline{a}_{ji} = 0 \quad \forall j \in \text{supp}(\widehat{\mathbf{C}}) \quad (25)$$

Proof.

$$\mathbf{0} = \mathbf{X}_{:,i} = \sum_{j=1}^d \overline{a}_{ji} \widehat{\mathbf{C}}_{:,j} + \mathbf{C}_{:,i} = \sum_{j \in \text{supp}(\widehat{\mathbf{C}})} \overline{a}_{ji} \widehat{\mathbf{C}}_{:,j} + \mathbf{C}_{:,i} \quad (26)$$

If $\mathbf{C}_{:,i} \neq \mathbf{0}$ then $i \in \text{supp}(\widehat{\mathbf{C}})$, and the expression above constitutes a linear combination of the support columns with not all coefficients non-zero. This contradicts Lemma B.8. Thus $\mathbf{C}_{:,i} = \mathbf{0}$ and $\overline{a}_{ji} = 0 \quad \forall j \in \text{supp}(\widehat{\mathbf{C}})$. \square

We are now ready to prove Prop. B.13.

Proof. We first choose a k -pair $\mathbf{C}, \widehat{\mathbf{C}}$ such that the support S of \mathbf{C} is concentrated to the last k columns, namely $\mathbf{C}_{:,i} = \mathbf{0}$ for $i = 1, \dots, d-k$. Then the corresponding data submatrix \mathbf{X} will necessarily have the same sparsity pattern since the values are computed according to predecessors, which in our case lie in smaller indices. Thus $\mathbf{X}_{:,i} = \mathbf{0} \quad \forall i = 1, \dots, d-k$ and according to Lemma B.15 we get that

$$\overline{a}_{ji} = 0, \text{ for all } 1 \leq i \leq d-k \text{ and } d-k+1 \leq j \leq d. \quad (27)$$

We notice that the desired condition is fulfilled for $i = d-k$, i.e. it has no non-zero influence from a node with larger index. We now prove the same sequentially for $i = d-k-1, d-k-2, \dots, 1$ by moving each time left the leftmost index of the support S . We prove the following statement by induction:

$$P(l) : \overline{a}_{ji} = 0 \text{ for } l < j, i < j \leq d-k \quad (28)$$

We know that $P(d-k)$ is true and $P(1)$ gives the required relation for all indices $i = 1, \dots, d-k$. Now we assume that $P(l)$ holds. If we pick k -pair $\mathbf{C}, \widehat{\mathbf{C}}$ such that \mathbf{C} has support $S = \{l, d-k+2, d-k+3, \dots, d\}$. Then $\mathbf{X}_{:,i} = \mathbf{0}$ for all $i < l$ which with Lemma B.15 gives $\mathbf{C}_{:,i} = \mathbf{0}$ for $i < l$ which means $\text{supp}(\widehat{\mathbf{C}}) \subset \{l, l+1, \dots, d\}$ and $\overline{a}_{ji} = 0$ for $j \in \text{supp}(\widehat{\mathbf{C}})$. Note, that by the induction hypothesis we have that $\overline{a}_{jl} = 0$ for all $l < j$. However it is true that $\mathbf{X}_{:,l} = \mathbf{C}_{:,l}$ and also

$$\mathbf{X}_{:,l} = \sum_{j \in \text{supp}(\widehat{\mathbf{C}})} \overline{a}_{jl} \widehat{\mathbf{C}}_{:,j} + \widehat{\mathbf{C}}_{:,l} = \widehat{\mathbf{C}}_{:,l} \quad (29)$$

Therefore $l \in \text{supp}(\widehat{\mathbf{C}})$ and thus $\overline{a}_{li} = 0$ for all $i < l$ which combined with $P(l)$ gives

$$\overline{a}_{ji} = 0 \text{ for } l-1 < j, i < j, i \leq d-k \quad (30)$$

which is exactly $P(l-1)$ and the induction is complete.

Now it remains to show that $\overline{a}_{ji} = 0$ for $d-k+1 \leq i \leq d$ and $i < j$. We will again proceed constructively using induction. This time we will sequentially choose support S that is concentrated on the last $k+1$ columns and at each step we will move the zero column one index to the right. For $l = d-k+1, \dots, d$ let's define:

$$Q(l) : \overline{a}_{jl} = 0 \text{ for } l < j \text{ and } \overline{a}_{jl} = \overline{a}_{jl} \text{ for } d-k \leq j < l \quad (31)$$

First we show the base case $Q(d-k+1)$. For this we choose a k -pair $\mathbf{C}, \widehat{\mathbf{C}}$ such that \mathbf{C} has support $S = \{d-k, d-k+2, d-k+3, \dots, d\}$. It is true that $\mathbf{X}_{:,i} = \mathbf{0}$ for $i = 1, \dots, d-k-1$ hence $\widehat{\mathbf{C}}_{:,i} = \mathbf{0}$ for $i \leq d-k-1$ and therefore the node $d-k$ doesn't have any non-zero parents, since also $\overline{a}_{j(d-k)} = 0$ for $d-k < j$ from previous claim. Therefore $\widehat{\mathbf{C}}_{:,d-k} = \mathbf{X}_{:,d-k} = \mathbf{C}_{:,d-k}$. Also, for $l = d-k+1$

$$\mathbf{X}_{:,l} = \overline{a}_{d-k,l} \mathbf{C}_{:,d-k} = \overline{a}_{d-k,l} \widehat{\mathbf{C}}_{:,d-k} \quad (32)$$

The equation from $\widehat{\mathbf{A}}$ gives:

$$\mathbf{X}_{:,l} = \sum_{j=d-k}^d \bar{a}_{jl} \widehat{\mathbf{C}}_{:,j} + \widehat{\mathbf{C}}_{:,l} \Rightarrow (\bar{a}_{d-k,l} - \bar{a}_{d-k,l}) \widehat{\mathbf{C}}_{:,d-k} + \sum_{j=d-k+1}^d \bar{a}_{jl} \widehat{\mathbf{C}}_{:,j} + \widehat{\mathbf{C}}_{:,l} = \mathbf{0} \quad (33)$$

From the linear Independence Lemma B.8 of the support of $\widehat{\mathbf{C}}$ we necessarily need to have $\widehat{\mathbf{C}}_{:,l} = \mathbf{0}$, $\bar{a}_{d-k,l} = \bar{a}_{d-k,l}$ and $\bar{a}_{jl} = 0$ for $l < j$ which gives the base case.

For the rest of the induction we proceed in a similar manner. We assume with strong induction that all $Q(d-k+1), \dots, Q(l)$ are true and proceed to prove $Q(l+1)$. Given these assumptions we have that

$$\bar{a}_{ji} = \bar{a}_{ji} \text{ for } d-k \leq j < i, d-k \leq i \leq l \text{ and } \bar{a}_{ji} = 0 \text{ for } i < j, d-k \leq i \leq l \quad (34)$$

Consider root causes support $S = \{d-k, d-k+1, \dots, l, l+2, \dots, d\}$ (the $(l+1)$ -th column is $\mathbf{0}$) for the k -pair $\mathbf{C}, \widehat{\mathbf{C}}$. Then we have the equations:

$$\begin{aligned} \mathbf{X}_{:,d-k} &= \mathbf{C}_{:,d-k} = \widehat{\mathbf{C}}_{:,d-k} \\ \mathbf{X}_{:,d-k+1} &= \bar{a}_{d-k,d-k+1} \mathbf{C}_{:,d-k} + \mathbf{C}_{:,d-k+1} = \bar{a}_{d-k,d-k+1} \widehat{\mathbf{C}}_{:,d-k} + \widehat{\mathbf{C}}_{:,d-k+1} \Rightarrow \widehat{\mathbf{C}}_{:,d-k+1} = \mathbf{C}_{:,d-k+1} \\ &\vdots \\ \mathbf{X}_{:,l} &= \sum_{j=d-k}^{l-1} \bar{a}_{jl} \mathbf{C}_{:,j} + \mathbf{C}_{:,l} = \sum_{j=d-k}^{l-1} \bar{a}_{jl} \widehat{\mathbf{C}}_{:,j} + \widehat{\mathbf{C}}_{:,l} \Rightarrow \widehat{\mathbf{C}}_{:,l} = \mathbf{C}_{:,l} \end{aligned}$$

Where we used the linear independence lemma and sequentially proved that the root causes columns up to l are equal. The equation for the $(l+1)$ -th column now becomes:

$$\mathbf{X}_{:,l+1} = \sum_{j=d-k}^l \bar{a}_{j,l+1} \mathbf{C}_{:,j} + \mathbf{C}_{:,l+1} = \sum_{j=d-k}^d \bar{a}_{j,l+1} \widehat{\mathbf{C}}_{:,j} + \widehat{\mathbf{C}}_{:,l+1} \quad (35)$$

$$\Leftrightarrow \sum_{j=d-k}^d (\bar{a}_{j,l+1} - \bar{a}_{j,l+1}) \widehat{\mathbf{C}}_{:,j} + \widehat{\mathbf{C}}_{:,l+1} = \mathbf{0} \Rightarrow \begin{cases} \bar{a}_{j,l+1} = 0 \text{ for } l+1 < j \\ \bar{a}_{j,l+1} = \bar{a}_{j,l+1} \text{ for } j < l+1 \\ \widehat{\mathbf{C}}_{:,l+1} = \mathbf{0} \end{cases} \quad (36)$$

where the last set of equalities follows from linear independence. This concludes the induction and the proof. \square

To complete the proof of Theorem B.1 it remains to show the following proposition.

Proposition B.16. *If both $\mathbf{A}, \widehat{\mathbf{A}}$ are upper triangular then $\widehat{\mathbf{A}} = \mathbf{A}$.*

For our proof we use the following definition.

Definition B.17. We denote by \mathcal{P}_k the set of all k -pairs $\mathbf{C}_R, \widehat{\mathbf{C}}_R$ for all possible support patterns.

Now we proceed to the proof.

Proof. We will show equivalently that $\widehat{\mathbf{A}} = \mathbf{A}$ using two inductions. First we show for $l = 1, \dots, k$ the following statement.

$P(l)$: For all k -pairs $\mathbf{C}, \widehat{\mathbf{C}}$ in \mathcal{P}_k the first l non-zero columns $\mathbf{C}_{:,i_1}, \mathbf{C}_{:,i_2}, \dots, \mathbf{C}_{:,i_l}$ and $\widehat{\mathbf{C}}_{:,i_1}, \widehat{\mathbf{C}}_{:,i_2}, \dots, \widehat{\mathbf{C}}_{:,i_l}$ are in the same positions, i.e. $i_j = \hat{i}_j$ and

- either they are respectively equal $\mathbf{C}_{:,i_j} = \widehat{\mathbf{C}}_{:,i_j}$
- or $\mathbf{C}_{:,i_l}$ is in the last possible index, namely $i_l = d - (l - 1)$

For the base case $P(1)$, consider a k -pair $\mathbf{C}, \widehat{\mathbf{C}}$ and let i_1 be the position of the first non-zero root causes column of \mathbf{C} . Then $\mathbf{X}_{:,i} = \mathbf{0}$ for $i < i_1$ and therefore from Lemma B.15 $\widehat{\mathbf{C}}_{:,i} = \mathbf{0}$ for $i < i_1$. Hence

$$\mathbf{X}_{:,i_1} = \sum_{j < i_1} \bar{a}_{ji_1} \widehat{\mathbf{C}}_{:,j} + \widehat{\mathbf{C}}_{:,i_1} = \widehat{\mathbf{C}}_{:,i_1} \quad (37)$$

Therefore $\widehat{\mathbf{C}}_{:,i_1} = \mathbf{C}_{:,i_1}$ and we proved $P(1)$, by satisfying both the positioning and the first requirement.

Assuming now that $P(l)$ holds, we will show $P(l+1)$. Take any k -pair of \mathcal{P}_k which we denote by $\mathbf{C}, \widehat{\mathbf{C}}$. Then, if $\mathbf{C}_{:,i_l}$ is in the last possible position, then necessarily $\mathbf{C}_{:,i_{l+1}}$ is in the last possible position. Moreover, from the induction hypothesis the first l root

causes columns are in the same positions. Therefore in the same manner, $\widehat{\mathbf{C}}_{:,i_l}$ is in the last position and $\widehat{\mathbf{C}}_{:,i_{l+1}}$, too. This case fulfills the desired statement.

If $\mathbf{C}_{:,i_l}$ is not in the last position, then from induction hypothesis, the first l root causes columns are equal. If $\mathbf{C}_{:,i_{l+1}}$ is in the last position and the same holds $\widehat{\mathbf{C}}_{:,i_{l+1}}$, the requirement is satisfied. Otherwise $\hat{i}_{l+1} < i_{l+1}$ and the equation for \hat{i}_{l+1} gives:

$$\mathbf{X}_{:,i_{l+1}} = \sum_{j=1}^l \bar{a}_{i_j, \hat{i}_{l+1}} \widehat{\mathbf{C}}_{:,i_j} + \widehat{\mathbf{C}}_{:,i_{l+1}} = \sum_{j=1}^l \bar{a}_{i_j, \hat{i}_{l+1}} \mathbf{C}_{:,i_j} + \mathbf{0} \Leftrightarrow \sum_{j=1}^l (\bar{a}_{i_j, \hat{i}_{l+1}} - \bar{a}_{i_j, i_{l+1}}) \widehat{\mathbf{C}}_{:,i_j} + \widehat{\mathbf{C}}_{:,i_{l+1}} = \mathbf{0}$$

According to linear independence Lemma B.8 we necessarily derive $\widehat{\mathbf{C}}_{:,i_{l+1}} = \mathbf{0}$, absurd. Thus $\hat{i}_{l+1} = i_{l+1}$ and the induction statement is fulfilled in that case.

It remains to consider the case where $\mathbf{C}_{:,i_{l+1}}$ is not in the last position. Since, i_{l+1} is not the last position there exists a k -pair \mathbf{C}' , $\widehat{\mathbf{C}}'$ such that the column i_{l+1} is zero and the $(l+1)$ -root causes column of \mathbf{C}' lies at $i'_{l+1} > i_{l+1}$. The equation at i_{l+1} for \mathbf{X}' gives:

$$\mathbf{X}'_{:,i_{l+1}} = \sum_{j=1}^l \bar{a}_{i_j, i_{l+1}} \mathbf{C}'_{:,i_j} = \sum_{j=1}^l \bar{a}_{i_j, \hat{i}_{l+1}} \widehat{\mathbf{C}}'_{:,i_j} + \widehat{\mathbf{C}}'_{:,i_{l+1}} \quad (38)$$

For the pair \mathbf{C}' , $\widehat{\mathbf{C}}'$ the induction hypothesis holds, thus we derive:

$$\sum_{j=1}^l (\bar{a}_{i_j, \hat{i}_{l+1}} - \bar{a}_{i_j, i_{l+1}}) \widehat{\mathbf{C}}'_{:,i_j} + \widehat{\mathbf{C}}'_{:,i_{l+1}} = \mathbf{0} \quad (39)$$

Therefore, Lemma B.8 gives $\bar{a}_{i_j, \hat{i}_{l+1}} = \bar{a}_{i_j, i_{l+1}}$ for all $j = 1, \dots, l$ and returning back to the equation for $\mathbf{X}_{:,i_{l+1}}$ we derive:

$$\mathbf{X}_{:,i_{l+1}} = \sum_{j=1}^l \bar{a}_{i_j, i_{l+1}} \mathbf{C}_{:,i_j} + \mathbf{C}_{:,i_{l+1}} = \sum_{j=1}^l \bar{a}_{i_j, \hat{i}_{l+1}} \widehat{\mathbf{C}}_{:,i_j} + \widehat{\mathbf{C}}_{:,i_{l+1}} \quad (40)$$

$$\stackrel{P(l)}{=} \sum_{j=1}^l \bar{a}_{i_j, \hat{i}_{l+1}} \mathbf{C}_{:,i_j} + \widehat{\mathbf{C}}_{:,i_{l+1}} \quad (41)$$

$$\Rightarrow \widehat{\mathbf{C}}_{:,i_{l+1}} = \mathbf{C}_{:,i_{l+1}} \quad (42)$$

which completes the induction step. Notice that $P(k)$ gives that for all k -pairs, the k root causes columns are in the same position. Given this fact we will now show that $\widehat{\mathbf{A}} = \mathbf{A}$. We will prove by induction that for $l = k-1, \dots, 1, 0$

$$Q(l) : \bar{a}_{i_j} = \bar{a}_{i_j} \text{ for } 1 \leq i < j < d-l \quad (43)$$

To prove $Q(k-1)$ we choose all the k -pairs \mathbf{C} , $\widehat{\mathbf{C}}$, such that $\mathbf{C}_{:,i_2}$ is in the last possible position, $i_2 = d-k+2$. Then for $i_1 \leq d-k$ the columns $\mathbf{C}_{:,i_1}$, $\widehat{\mathbf{C}}_{:,i_1}$ lie at the same position and are equal. Choosing $i_1 = i$ and computing the equation for $\mathbf{X}_{:,j}$ where $i < j \leq d-k+1$ gives:

$$\mathbf{X}_{:,j} = \bar{a}_{i_j} \mathbf{C}_{:,i} = \bar{a}_{i_j} \widehat{\mathbf{C}}_{:,i} = \bar{a}_{i_j} \mathbf{C}_{:,i} \quad (44)$$

Therefore $\bar{a}_{i_j} = \bar{a}_{i_j}$ for all $1 \leq i < j \leq d-(k-1)$ and $Q(k-1)$ is satisfied. Next, assume that $Q(k-l)$ is true. We want to show $Q(k-l-1)$. Similarly to the base case we consider all k -pairs such that $\mathbf{C}_{:,i_{l+2}}$ lies in its last possible position $i_{l+2} = d-k+l+2$, and $i_{l+1} \leq d-k+l$. Since the $(l+1)$ -th column is not in the last position, from the previous induction we have that:

$$\begin{cases} \widehat{\mathbf{C}}_{:,i_1} = \mathbf{C}_{:,i_1} \\ \widehat{\mathbf{C}}_{:,i_2} = \mathbf{C}_{:,i_2} \\ \vdots \\ \widehat{\mathbf{C}}_{:,i_{l+1}} = \mathbf{C}_{:,i_{l+1}} \end{cases} \quad (45)$$

The equation for $d-k+l+1$ gives:

$$\mathbf{X}_{:,d-k+l+1} = \sum_{j=1}^{l+1} \bar{a}_{i_j, d-k+l+1} \mathbf{C}_{:,i_j} \quad (46)$$

$$= \sum_{j=1}^{l+1} \bar{a}_{i_j, d-k+l+1} \widehat{\mathbf{C}}_{:,i_j} \quad (47)$$

$$= \sum_{j=1}^{l+1} \bar{a}_{i_j, d-k+l+1} \mathbf{C}_{:,i_j} \quad (48)$$

$$\stackrel{\text{Lemma B.8}}{\Rightarrow} \bar{a}_{i_j, d-k+l+1} = \bar{a}_{i_j, d-k+l+1} \quad (49)$$

By choosing all such possible k -pairs the indices i_j span all possibilities $1 \leq i < d - k + l + 1$. Combining this with $Q(k - l)$ we get that $Q(k - l - 1)$ is true and the desired result follows. \square